PAPR REDUCTION IN OFDM-BASED NOMA USING TRELLIS SHAPING

By

NS Sara Fiaz

(00000275833)

A thesis submitted to the faculty of Electrical Engineering Department,
Military College of Signals, National University of Sciences and Technology,
Islamabad, Pakistan, in partial fulfillment of the requirements for the degree of MS in
Electrical (Telecommunication) Engineering

August 2022

THESIS ACCEPTANCE CERTIFICATE

Certified that final copy of MS Thesis written by NS Sara Fiaz,Registration No. 00000275833, of Military College of Signals (MCS)has been vetted by undersigned, found complete in all respect as per NUST Statutes/Regulations, is free of plagiarism, errors and mistakes and is accepted as partial, fulfillment for award of MS degree. It is further certified that necessary amendments as pointed out by GEC members of the scholar have been also incorporated in the said thesis.

Signature:_____

Name of Supervisor: Asst Prof Abdul Wakeel, PhD

Date:_____

Signature (HoD): _____

Date: _____

Signature (Dean): _____

Date:_____

DECLARATION

I confirm that the work presented in this thesis, ”PAPR reduction in OFDM-based NOMA using trellis shaping,” has not been submitted in support of any other award of educational qualification at this institute or elsewhere.

_____

NS Sara Fiaz

00000275833

COPYRIGHT STATEMENT

DEDICATION

This thesis is dedicated to

MY FAMILY, FRIENDS AND TEACHERS

for their love, endless support and encouragement

ABSTRACT

Wireless communication networks are expanding exponentially which makes challenging requirements for 5-generation (5G) and beyond 5G wireless technology. Different solutions have been proposed by the researchers to fulfil these demanding challenges. One of such technique which is making its way into 5G communication technologies is non-orthogonal multiple access (NOMA). NOMA has been considered as possible radio access mechanism for the next-generation of cellular networks. The system performance can further be enhanced using OFDM-Based NOMA. However, a major drawback of multicarrier NOMA is its inherited high peak-to-average power ratio (PAPR). OFDM-based NOMA systems with a high PAPR are inefficient in terms of energy use. Herein, we propose Trellis for PAPR reduction in OFDM-based NOMA systems. Trellis shaping is a distortion-free techniques which provides promising gains in terms of PAPR reduction. The metric used to search for a sequence of symbols (shaped symbols) in the trellis of the shaping code is based on minimization of the auto-correlation of the side lobes. This method's performance is based on constellation mapping. Simulation results obtained shows that a promising gain in terms of PAPR can be obtained with our proposed solution for OFDM-based NOMA systems. To boost the system's performance in terms of PAPR, we further propose the use of higher-depth shaping codes. Using shaping codes with higher trellis depths improves the PAPR reduction.

As second part of this thesis, we propose a hybrid PAPR reduction algorithm: active constellation extension based trellis shaping for PAPR reduction in OFDM-based NOMA systems. Extending the constellation points provides additional gains in terms of PAPR.

ACKNOWLEDGEMENTS

I am grateful to Almighty for providing me with the motivation and strength to complete my thesis; without His kindness and mercy, I would not have taken on this work.

The achievement of this thesis is accomplished with the participation and cooperation of al guidance committee. With deep appreciation, i acknowledge our indebtedness to honorable supervisor Dr. Abdul Wakeel, who encouraged my spirits at critical junctures supported me with every possible guidance which led to the successful completion of this work. The accomplishment of this thesis also involved the cooperation and participation of all the guidance committee members.

I want to offer my heartfelt gratitude to my wonderful parents for their unwavering support and encouragement. Last but not least, I am grateful to the Electrical Engineering Department faculty members at MCS for their guidance and support throughout my time at the college.

TABLE OF CONTENTS

LIST OF FIGURES

ACRONYMS

Multiple Access	MA
Code Division Multiple Access	CDMA
Non- Orthogonal Multiple Access	NOMA
Orthogonal Frequency Division Multiple Access	OFDMA
Radio Access	RA
Orthogonal Frequency Division Multiplexing	OFDM
Frequency Division Multiplexing	FDM
Inter-Symbol Interference	ISI
$\mathcal{M}$ Quadrature Amplitude Modulation	$\mathcal{M} - QAM$
Inverse Discrete Fourier Transform	IDFT
Inverse Fast Fourier Transform	IFFT
Discrete Fourier Transform	DFT
Cyclic Prefix	CP
Equalizer	EQ
Channel State Information	CSI
Successive Interference Cancellation	SIC
User Equipment	UE
Superposition Coding	SC
Base Station	BS
Non-Linear Distortion	NLD
Selected Mapping	SLM
Partial Transmit Sequence	PTS
Tone Reservation	TR
Peak-to Average Power Ratio	PAPR
Bit Error Rtae	BER
Walsh Hadamard Transform	WHT
Zadoff chu Transform	ZCT
Frequency Selective Fading	FSF
Discontinuos Hartley Transform	DHT

Spectral Efficiency	SE
Tone Injection	TI
Linear Program	LP
Signal to Noise Ratio	SNR
Complementary Cumulative Distribution Function	CCDF
Phase Shift Keying	PSK
Zero Forcing	ZF
Minimal Mean Square Error	MMSE
Discrete Multi Tone	DMT
Far End User	FEU
Peak Reduction Tone Fraction	PRTF
Multi Carrier Modulation	MCM
Central Limit Theorem	CLT
High Power Amplifier	HPA
Input Power Back-off	IBO
Trellis Shaping	TS
Peak-to-Average Power Ratio	PAPR
Active Constellation Extension	ACE
Triangular Quadrature Amplitude Modulation	$\mathcal{T} - QAM$

Chapter 1

Introduction

1.1 Background

Wireless communication systems have been evolved drastically in the last few decades. Different communication technologies such as 1G, 2G, 3G, 4G, and 5G and beyond 5G wireless communication systems were proposed or deployed. Due to the advent of numerous mobile applications, video conferencing, and online gaming, there is an increased demand for higher data rates. To meet the public demand for higher data rates, researchers have developed novel multiplexing and transmission strategies, that make use of the available resources resources efficiently. NOMA is one of these strategies, paving its way into 5G communication technologies. As opposed to orthogonal multiple access (OMA), the orthogonality restriction is relaxed in NOMA where several users share the same resource block [1].

Recently, NOMA is hot topic and has actively been researched. Different variants have been proposed which can broadly be divided into two categories: power-domain (PD-NOMA) [2] and code-domain (CD-NOMA) [3]. In PD-NOMA, several users can be served in the same time slot, OFDMA sub-carrier, or spreading code, and multiple accesses are achieved by assigning different power levels to the multiplexed users. Moreover, PD-NOMA assign high power to the user having poor channel condition and less power to the user having good channel condition. In CD-NOMA, two users are served with the same code in the same resource block. The code CD-NOMA differs significantly from that of CDMA. In reality, CDMA is based on the premise that users may be distinguished by the differences in their spreading codes, whereas NOMA urges multiple clients to use the same code.

NOMA-based OFDM (NOMA-OFDM) will be the ideal solution for 5G communication

systems to improve system performance in terms of resource usage. Using the same resource block, OFDM will give robustness against channel impairments, whereas NOMA will provide massive connectivity. However, a major disadvantage of multicarrier systems is that it has high PAPR in time domain. In a multicarrier OFDM system, the sub-carriers are independent and identically distributed (i.i.d.) which, according to the Central Limit (CL) theorem, results in a Gaussian-like distribution with a high PAPR, . When such as signal is passed through a non-linear device such as high power amplifier (HPA), analog-to-digital converter (ADC), e.t.c., it will drive the non-linear device to operate in its non-linear region resulting in the transmit signal is clipping. This causes distortion within the band (in-band distortion) which reduces the system's bit error rate performance, as well as out-of-band radiation, which results in inter symbol interference. Countermeasures needs to be taken to avoid signal clipping by the non-linear circuitaries. One possible approach is to operate the non-linear devices with larger back-up voltages; however, this is inefficient because the high peaks are irregular and the signal amplitude remains low for the majority of time. Therefore, altenative solutions are to use different PAPR reduction strategies to limit the peak power excursions of the time domain transmit signal. To limit the high PAPR, various techniques have been proposed in the literature for the conventional OFDM systems. However, few attempts have been made so far for the PAPR reduciton in NOMA-OFDM systems.

For the conventional OFDM systems, Clipping [4], is the simplest techniques in which the signal is clipped whenever its peak amplitude exceeds a given threshold. However, Clipping has a number of disadvantages including the in-band disruption and out-of-band emission. The in-band disruption leads to a decrease in performance in terms of high BER, which can be mitigated by utilizing various error correction coding. To further improve the clipping technique, Clipping and Filtering approach was proposed in [4] which helps in mitigating the effect of out-of-band radiation. In Selected mapping SLM [14] multiple copies of the same

OFDM frame are created using different phasor vectors and the one with the lowest PAPR is considered for transmission. SLM, on the other hand, is computationally demanding and necessitates the communication of side information about the phasor to the receiver. Muller and Huber, in [14], proposed partial transmit sequences (PTS) which is another well-known strategy for PAPR reduction. PTS works on the same idea as Selected Mapping, i.e., multiple signal representations containing the same information. PTS divides the information bearing frame into separate sets and applies the phasor vectors to each sub block separately. The transmission of a mixture of these sub blocks with a low PAPR is then chosen. PTS has slightly better performance than SLM, however, it comes with additional computational complexity. Tellado proposed the Tone Reservation (TR) technique for PAPR reduction in [15]. It is the simplest of the PAPR reduction algorithms. TR divides an OFDM frame's total sub-carriers into two sets, one set of sub-carriers is utilized for data transmission, while the other set is employed to generate a corrective function, which is then used iteratively in time domain to limit the transmit peak excursion of the signal. Pre-coding-based solutions show promise behavior since they are simple to implement and do not require any extra information to be sent with the transmitted signal [12]. A significant variety of techniques have been proposed to resolve the PAPR problem in OFDM-based systems [9] [10] [11]. In [12], the Walsh Hadamard transform (WHT) is used for the first time to resolve the issue of high PAPR in OFDM systems. Similarly, Zad-off-chu sequences has been studied for OFDMA systems to reduce PAPR [13]. The discrete Hartley transform (DHT), another pre-coding approach, has also shown promise in lowering PAPR.

Trellis shaping (TS) is considered to be a very efficient PAPR reduction technique in the literature. TS was first proposed by Forney's in [6], where the author used Viterbi algorithm to efficiently minimize the average power of $\mathcal{M} - QAM$ signals. Later on, the idea of TS was extended for PAPR reduction by Henkel and Wagner in [7], where the authors showed

that TS may be used to reduce the high peak power of OFDM signals. Werner proposed two metrics, one each for time and frequency domains. The authors showed in [7] that the time domain metric has high PAPR reduction capability at the expense of computational complexity. In [16], Ochiai extneded the TS idea and proposed a frequency domain metric for the search in the viterbi algorithm based on the minimization of the autocorrelation of the side lobes.

In conventional OFDM systems, the aforementioned strategies have been extensively used for PAPR reduction, however, relatively little work has been done in NOMA-based OFDM systems. A first approach was made by Arsala Khan et al. in [17], where the authors have proposed the first method for reducing PAPR in NOMA-OFDM systems. To tackle the PAPR problem in downlink NOMA, a pre-coded NOMA system was presented in [17]. In NOMA, various unitary transforms such as the Walsh Hadamard transform (WHT), Zadoff chu transform (ZCT), and discontinuous Hartley transform are used to resolve the PAPR problem. T-transform, a hybrid of WHT and ZCT, was also suggested as a novel pre-coding technique in [19]. Herein, we propose a modified TS algorithm for PAPR reduction in NOMA-based OFDM systems. We also propose a hybrid scheme; Active Constellation Extension (ACE) based trellis shaping for PAPR reduction in NOMA-OFDM systems.

1.2 Problem Statement

OFDM is considered as a possible candidate for future communication system due to its robustness against multiple path fading. Moreover, NOMA relaxes the orthogonality constraint which helps the future communication systems to provide massive connectivity. Thus, NOMA-OFDM are considered as a running candidate for 5G and beyond communication systems. However, a major drawback of NOMA-OFDM is its high PAPR, which is limiting its way to be deployed as a connected service in future wireless communication systems.

Transmit signal with sporadic high peaks when passed through non-linear devices, such as HPA, ADC, e.t.c., will drive them to operate in their non-linear regions, which, thus, results in signal clipping. Clipping distorts the signal and results in system performance degradation. Therefore, countermeasures need to be taken before passing such a signal through the non-linear devices. Different approaches has been made by different researchers in the literature to limit these peak excursions. Herein, we propose TS for PAPR reduction in down-link PD NOMA-OFDM systems. To keep the peak excursion to a minimum, TS is one of the greatest approaches available in literature for PAPR reduction in multicarrier systems. As compared to SLM, PTS, TR and clipping, TS shaping provides best results in terms of PAPR reduction without signal distortion for average computational complexity [2]. Moreover, TS does not increase the mean transmit power as it did in the case of TR [1]. To further improve system's effectiveness, higher trellis-depths shaping codes are used in TS. Beside TS, a hybrid scheme: ACE-based TS for PAPR reduction in NOMA-OFDM is proposed which further improves the system performance for a marginal increase in the mean power.

1.3 Objectives

The goal of this study is to accomplish the following objectives:

1. To evaluate and analyse TS as possible solution for PAPR reduction in NOMA-OFDM systems which helps in improving the system performance.

2. To evaluate the proposed scheme's performance considering shaping codes of various trellis depths.

3. To analyse the formance of a hybrid PAPR reduction algorithm, i.e., Active Constellation Extension based Trellis Shaping for PAPR reduction in NOMA-OFDM systems.

1.4 Contributions

PAPR reduction is a hot area of research. Different PAPR reduction approaches, including as clipping and filtering, SLM, PTS, and TR, have been presented in the past for conventional SISO-OFDM systems. A first approach for PAPR reduction in NOMA-OFDM systems was made in [2], where the authors have employed Linear Pre-coding Techniques. The main contributions of this research work are

1. We propose and evaluate Trellis shaping for PAPR reduction in down-link PD NOMA-based OFDM systems, which is not available in the literature, to the best of our knowledge, and thus makes this study particularly unique. Simulations have been carried out to evaluate the performance of NOMA-OFDM system in terms of PAPR reduction.

2. This study also comprise of the use of different shaping codes with higher trellis depths in the TS algorithm to further improve the system performance.

3. As a third contribution, a hybrid scheme: ACE-based TS is proposed for PAPR reduction in NOMA-OFDM systems. Simulation results are provided which show the effectiveness of our proposed hybrid scheme.

1.5 Road Map

This thesis is organized in six chapters:

- **Chapter 1:** comprises of introduction and objectives as well as the contributions that we have made in this report

- **Chapter 2:** includes some preliminaries and background about NOMA, OFDM and OFDM-NOMA systems. It also provides brief summary of the already existing PAPR reduction techniques.

- **Chapter 3:** provides details about PAPR, quantitative measurement of PAPR, consequence of high PAPR and different PAPR reduction techniques available in the literature.

- **Chapter 4:** presents our suggested OFDM-based NOMA system model using TS for PAPR reduction. Moreover, it also provides the simulation results obtained with our proposed approach. The chapters also discusses the effect of using higher trellis depths shaping codes on PAPR reduction.

- **Chapter 5:** introduces our proposed hybrid PAPR reduction algorithm: ACE-based TS for PAPR reduction in OFDM-NOMA systems to enhance system's performance in terms of PAPR. The simulation results provided shows a substantial gain in terms of PAPR using the hybrid scheme.

- **Chapter 6:** concludes our investigation as well as pointing out some potential for future works.

Chapter 2

OFDM-NOMA

2.1 Orthogonal Frequency Division Multiplexing

Orthogonal frequency division multiplexing (OFDM) is a multi-carrier communication system with orthogonal sub-carriers. OFDM is used for high speed data transmission over noisy channels, reliably. It involves dividing a wide-band channel into a set of orthogonal, sequential, narrow-band sub-channels, which are ideally independent. Each sub-carrier is individually modulated using any digital modulation scheme, i.e., QPSK, $\mathcal{M}$-QAM, e.t.c.. Information is carried by these closely spaced orthogonal sub-carriers. The symbol rate is kept low so that it stays similar to the conventional single-carrier modulation technique. The symbol duration in OFDM is increased to combat the inter symbol interference (ISI). OFDM has diverse applications in in wireless communication networks, 4G/5G mobile communication, and digital video and audio broadcasting. Furthermore, OFDM has a lot of advantages, e.g., it is highly spectral efficient, resource allocation can be done flexibly, as well as OFDM is resistant to ISI. Because of its ability to deal with difficulties like multi-path propagation and higher data rates, OFDM is extremely important to spectral efficiency and data rates. A complete description about evolution of the OFDM systems can be found in [22, 23].

2.1.1 Basic Principle of OFDM System

Data bits streams are mapped on multiple carriers simultaneously in OFDM. This approach divides the transmission frequency band into a number of sub-bands, with the spectrum of each data symbol occupying one of them. [24] [25]. To reduce ISI between the sub-channels, the number of sub-channels are chosen in such a way that bandwidth of the sub-channel is

less than the coherence bandwidth of the channel. For better utilization of the bandwidth, OFDM allows frequency spectrum of an individual sub-carrier to overlap.

Binary data from a data source is encoded using a forward error correction (FEC) code at the transmitter. The encoded serial data stream is subsequently passed through the symbol mapping block, where the encoded data is modulated using different modulation schemes such as QPSK, $\mathcal{M}$-QAM, and others. The modulated $\mathcal{M}$-QAM symbols are then passed from a serial to parallel converter (S/P). After S/P, the modulated symbols are sent to the IFFT block where these modulated symbols are converted into time domain signal. ISI is significantly reduce by introducing a guard band between the OFDM symbol. After adding a guard interval to the time domain signal, the parallel data is subsequently transformed to serial data stream using a parallel-to-serial (P/S) converter and is the serial data stream is passed through a digital-to-analog converter (DAC) block which converts the digital signal into an analogue signal. The analogue signal is the transmitted via the transmitter antenna. The signal is received at the receiver's end, and the carrier synchronizer performs carrier synchronization. Through the use of a analog-to-digital (ADC) converter, these signals are transformed back to the digital form. Afterwards, the guard removal block and the time synchronizer block are responsible for guard removal and time synchronization, respectively. The time domain signal is converted into frequency-domain signal using an FFT block, which perform this operation on the signal received at the receiver after removal of the guard interval from the received signal. After converting the signal into frequency domain, channel estimation is done using equalizer on the frequency domain signal. After channel estimation, de-modulation is performed on the estimated symbols for demodulation, using the same schemes that were used at the transmitter end. Through a P/S converter, the parallel data stream is transformed into serial data. Finally, decoder is used to do bit decoding to decode the transmitted information.

2.1.2 Discrete Time OFDM Model

System model of a DT-OFDM is as shown in fig. 2.1 where the input bits are mapped first to the $\mathcal{M}$-ary QAM symbols

$$\mathbf{X} = [X_n] \qquad n = 1, 2, \cdots, N. \tag{2.1}$$

where $[X_n]$ is the nth sybmol written as

$$X_n = X_I(j) + X_Q(j) \tag{2.2}$$

The data rate and channel parameters are the only factors that determine the M-ary QAM constellation to use. Another advantage of OFDM is that the same QAM constellation isn't required for all $[X_n]$, therefore, several modulation can be utilized at the same time. Bit loading and power loading are two resource allocation strategies that are employed in different modulation schemes. After mapping, the M-ary QAM symbol is sent to a S/P converter, where the sequential data stream $[X_n]$ is converted into an equivalent data steam $[X_n]$. An IDFT (IFFT) modulator is used for converting the OFDM frame into time domain.

$$[x_k] = \text{IDFT}[X_n] = \frac{1}{\sqrt{N}} \sum_{n=1}^{N} X_n e^{j} \frac{2\pi nk}{N} \qquad k = 1, 2, \cdots, N\ . \tag{2.3}$$

After IFFT, P/S converter converts the time domain samples into serial data stream. The OFDM signal is augmented with CP before transmission to combat ISI having length μ. First, at the receiver, the cyclic prefix is removed, and the signal $\mathbf{y}_k$ is converted from a serial to a parallel data stream. The symbol's DFT is obtained. Finally, the obtained symbols are decoded as follows:

$$[Y_n] = \text{DFT}[\mathbf{y}_k] = \frac{1}{\sqrt{N}} \sum_{k=1}^{N} x_k e^{-} j \frac{2\pi nk}{N} \qquad n = 1, 2, \cdots, N \tag{2.4}$$

The orthogonality condition must be met in order for the detected symbol to be demodulated at the receiver, i.e., $T_s \delta f = 1$, the transmitted signal $x_{n,k}$ is received

$$x_{n,k} = \frac{1}{T_s} \int_0^{T_s} x_n(t) e^{-j2\pi k \Delta f t} dt \tag{2.5}$$

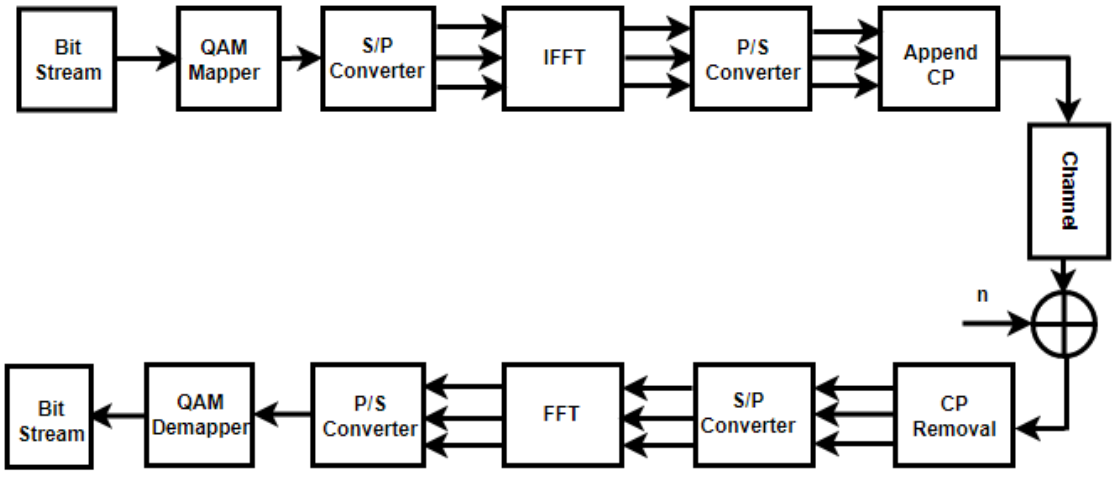

Figure 2.1: Block Diagram of OFDM

2.2 Non-Orthogonal Multiple Access

Conventional OMA techniques have facilitated users in the utilization of orthogonal resources. It can only serve a single user in a particular time slot or resource block. Due the orthogonality constraint, it cannot handle a large number of users with limited orthogonal resources. As future communication technologies aim for massive connectivity, therefore, OMA technologies and their performance is not compatible with the requirements of 5G communication. NOMA, on the other hand, are well suited to offer massive connectivity as a requirement due to spectrum scarcity in 5G technology, as they address vast connections with limited resources. Essentially, the NOMA method allows different users to share the same available resource by sending their data over the same channel at the same time. For example, in CD-NOMA, non orthogonal can be achieved by by employing user-specific

signatures while transmitting and receiving data. The reception device on the receiving end exploits the non-orthogonal sequences assigned to individual users on the broadcasting side in a multi-user detection system. Normally, devices are constrained by scheduling requests to transmit their data, however, researchers considers NOMA for grant-free transmission to see the possibilities of handling huge connections. Many variations of the NOMA principle have been offered in recent literature, all of which are based on its two essential categories: power-domain NOMA and code-based NOMA. Herein, otherwise stated, we will be considering power domain NOMA.

2.2.1 Basic Principle of NOMA

NOMA is a multiple access approach used in 5G. The main purpose of NOMA is that BS provides services to multiple users. It serves multiple customers at the same time and frequency block. At the transmitter end, superposition coding is carried out by superimposing multiple signals and successive interference cancellation (SIC) is being performed at the receiver end.

Figure 2.2 shows a block diagram of a typical power doamin NOMA system. As shown in the figure, two users U_{E_1} and U_{E_2}, generate binary data in the form of 0's and 1's. The data generated by U_{E_1} and U_{E_2} is passed through a modulation block where $\mathcal{M} - QAM$ Modulation is being performed. After modulation, each user is assigned different power levels on the basis of their distance from the central base station (BS). A user closer to BS is allocated less power and the user which is far from the BS is allocated more power. After power allotment, superposition coding is being performed where the signals from both the users are superimposed and transmit as a single signal. In NOMA-OFDM, this superimposed signal in S/P converted and is passed an IFFT modulator to convert it inot a TD signal. After converting signal into time domain, a guard interval known as cyclic prefix is appended

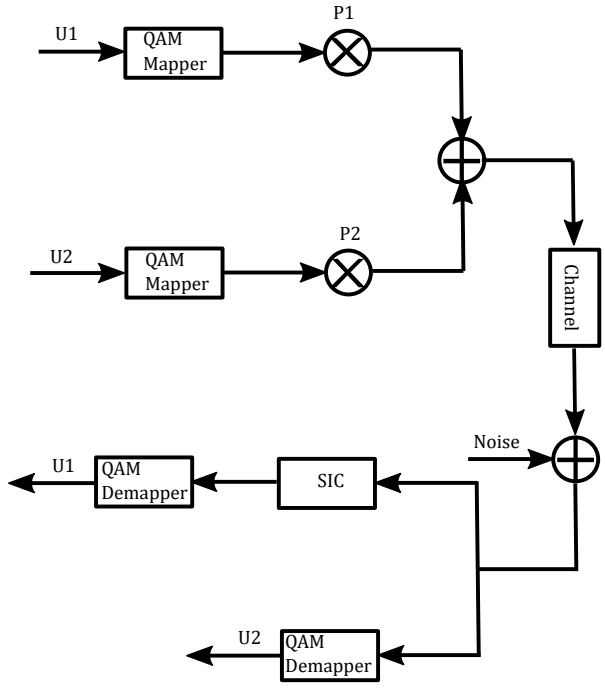

Figure 2.2: Block Diagram of NOMA

to the transmit signal which help in minimizing the effect of ISI. After adding the CP, the signal is transmitted over an additive white Gaussian noise (AWGN) channel where noise is added. At the receiver, reverse operations are performed till the FFT block. After FFT block, i.e., conversion from TD to FD, SIC is carried out at the user who has less power and the other user's data is transmitted to demodulation block where QAM-demodulation takes place and we get the desired data of that user. After performing SIC the data is transferred to demodulation and get the desired data of that user.

2.2.2 Superposition Coding and Successive Interference Cancellation

Transmitter use superposition coding (SC) to multiplex two users, whereas at the receiver, Successive Interference Cancellation (SIC) is used to extract each users data. At the transmitter side, all the signals containing information are superimposed into a single waveform, whereas SIC perform decoding on each signal till it gets the required signal at receiver. The strongest signal is the first one to be decoded using SIC considering the rest as interference's. In the later stages of SIC decoding, the signal that is decoded first is subtracted

from the received signal to decode the signal for the remaining users. If the decoding is performed without any error, the remaining signal from the waveform is perfectly obtained. This process is repeated until we get the signal for all the multiplexed users.

The success of SIC depends on how we perform signal cancellation in each iteration step. Power between the users should be accurately divided by the transmitter. Power allocation algorithm is different for both uplink and downlink NOMA.

2.2.3 Power-Domain NOMA

In PD-NOMA, powers of different level are allocated to users as their signatures. These power levels are determined on the distance between the BS and users. At the receiver side, utilizing successive-interference cancellation the users data are extracted. The PD-NOMA concept was first introduced in 2013 [40, 41, 42, 43, 44], allowing many users to share the same time-frequency resource at the same time, hence, improving the spectral efficiency of the wireless networks. Power domain NOMA is further categorized as Downlink-NOMA and Uplink-NOMA. Here we are restricted to Downlink-NOMA. In the next section we will be discussing about Downlink-NOMA. [40,41,42,43,44]. Next section discusses both these terms in detail.

Down-link PD-NOMA

In down-link PD-NOMA, SC is done at the transmitter whereas SIC is performed at the receiver side as shown in Fig. 2.2.3. Consider a central base station (BS) with two users U_{E_1} and U_{E_2}. Every user receives a certain portion of power based on its distance from the BS at the same time. Let's U_{E_1} lies close to the BS, whic would mean that it is in the higher SNR region, has a high channel gain, and has superior channel conditions. Therefore, U_{E_1} is assigned small portion of the total power P_T, i.e., $P_1 = \alpha P_T$. Similarly, if U_{E_2} lies farthest from the BS, it will have worst channel condition is assigned to the low SNR zone. U_{E_2} is

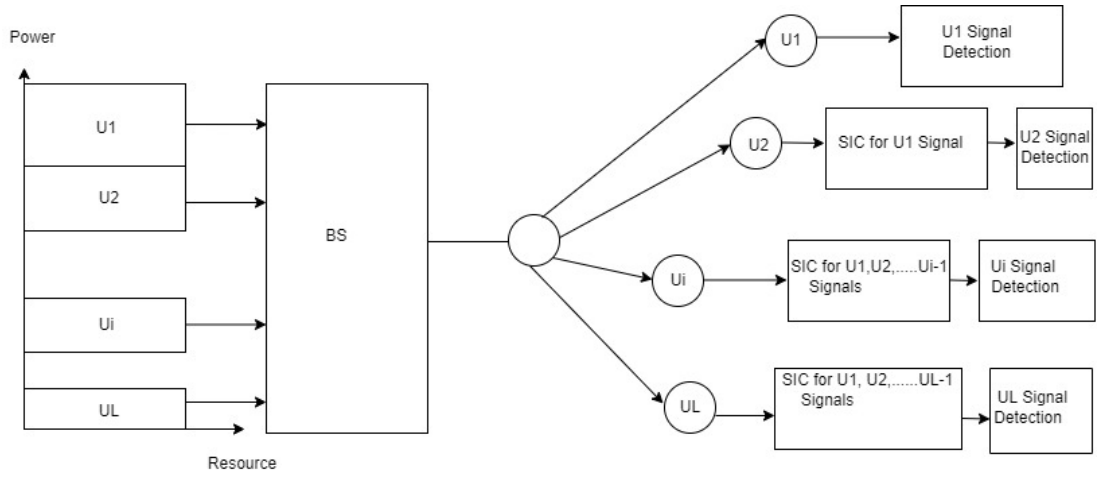

Figure 2.3: Downlink NOMA Network

therefore assigned high power as compared to U_{E_1}, i.e., $P_2 = (1 - \alpha)P_T$.

In down-link PD-NOMA, the BS superimposes wave-forms containing information for its serviced clients. At the receiver side, each user detects its own signal by employing SIC. The network consists of BS and K number of clients referred as U_{Es} as shown in Fig. 2.2.3. U_{E_1}, the user that is close to the BS and let U_{E_k} is the user that is far from the BS. Deciding how to distribute power among different clients is a challenging task for BS, which is important for SIC because if we don't know the power we are unable to perform SIC and unable to extract the signal error free. In Downlink-NOMA, high power is assigned to the user that is located further from the BS, whereas the user that is close to the BS is assigned less power. Every user in the network receives the same signal, containing data for all users. Each user starts by decoding the strongest signal first, and then subtracts it from received signal. Subtraction is repeated until the SIC receiver finds its own signal. Signals from U_{Es} further away can be cancelled by U_{Es} closer to the BS.

Power Allocation in Downlink NOMA

The issue for BS is selecting how to distribute power among a large number of information wave-forms, which is critical for SIC. The U_{Es} placed distant from the BS receive greater power in down-link NOMA, whereas the U_{Es} that has a less distance from the BS receives less power. Every U_{E_i} in the network gets the same signal, which contains data for all the users. Decoding of the signal starts for the user that has worst channel condition and containing more power and then subtracting it from the signal received. This cycle is repeated until the SIC receiver detects all the desired signal. U_{E_i} that has less distance from the BS can cancel signals from U_{Es} that has more distance from the BS. Because the signal from the U_{E_i} that has more distance contributes the most to the signal we received at the receiver, it is decoded first. The signal we get at the transmitter side by the BS is represented as:

$$x(t) = \sum_{k=1}^{K} \sqrt{\alpha_k} P_T x_k(t) \ , \tag{2.6}$$

where the individual waveform for transmitting information is $x_k(t)$, the power allocation coefficient is α_k , and the power available at the base station is P_T. The power allotted to each U_{E_K} at this time is $P_k = kP_T$. The power is divided based on the distance between the U_{Es} and the BS. U_{E_1} is the closest to the BS and thus receives the least power whereas U_{E_K} is the farthest and therefore receives the most power. The signal we received at U_{E_K} is represented as:

$$y_k(t) = x(t)g_k + w_k(t) \ , \tag{2.7}$$

where $g_k$is the channel attenuation factor for the BS-to-U_{E_K}, $w_k(t)$ is the additive white Gaussian noise at U_{E_K} with mean zero and spectral density N_0(W/Hz).

2.2.4 Code Domain NOMA

Code domain is the second main category of NOMA schemes, in which sharing of the same time-frequency resources by multiple users is done using unique spreading sequences. Al-

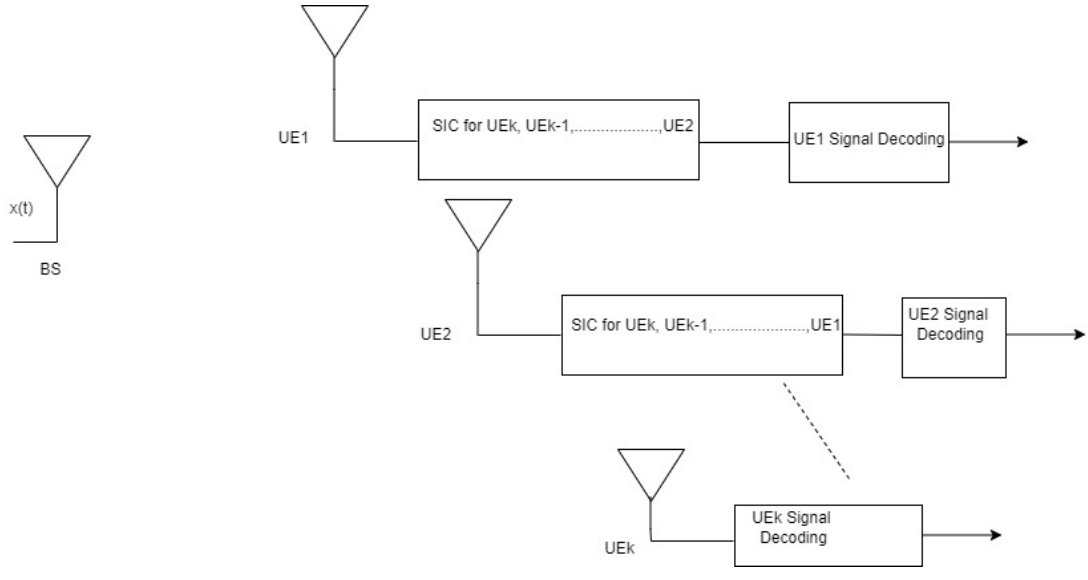

Figure 2.4: Power Allocation in NOMA

though, the concept is inspired from the typical CDMA, however, there is a difference in the code-domain NOMA as it has non-orthogonal or sparse and low cross-correlated spreading sequences [59]. Two main components can be used at the receiver of code-domain NOMA, i.e., an SIC for separating users and message passing algorithm (MPA) technique for multiple user detection [60]. Figure 2.2.4 shows system model of CD-NOMA.

2.3 OFDM-based NOMA

NOMA-based OFDM is one of the most capable technology for the next generation of communication. It is a viable way out to attain capacity gain over OMA-based OFDM. It has the potential to significantly boost data rate and spectral efficiency. A block diagram of downlink PD NOMA-OFDM system is as shown in Fig. 2.6. Users data is first mapped using $\mathcal{M}-QAM$ mapper and is assigned with different power levels. After superposition coding, the data is passed from a S/P converted and is transformed into time domain using an IFFT

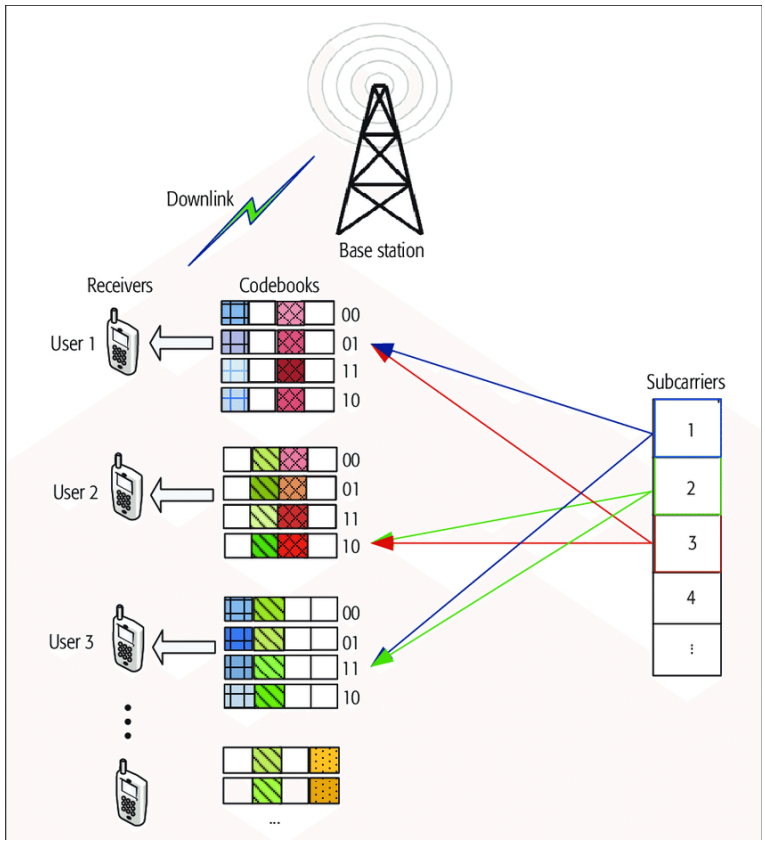

Figure 2.5: System Model of CD-NOMA

modulator. A CP is appended with the transmit signal to combat the effect of multi-path fading and ISI and is transmitted over the channel. At the receiver side, reverse operations are done to recover the recover the data transmitted.

One of the most important issue that OFDM-based system suffers is their high PAPR, which causes the HPA to operate in its non-linear region. Operating the HPA in non-linear region will clip the signal resulting in degradation of the system's performance. To overcome the problem of high PAPR in NOMA-based OFDM systems, different approaches have been made. In [60], to tackle the problem of high PAPR, a strategy based on pre-coding and dummy sequence insertion (DSI) was presented. In [61], a novel pre-coding method with Zadoff-Chu matrix transform (ZCT) is proposed to overcome this problem of high PAPR. In [62], the author propose a method to overcome the previous limitations, a low complexity PTS-based method based on the dummy sequence insertion (DSI) technique and the cyclic

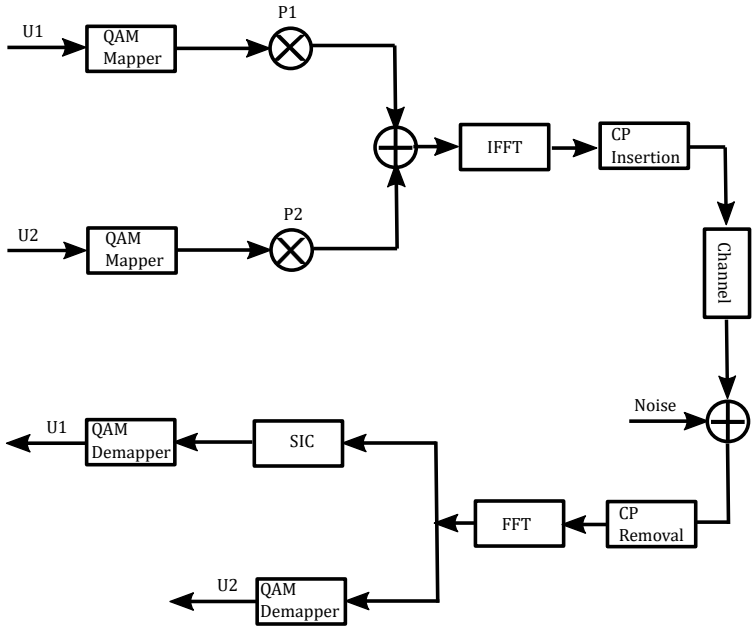

Figure 2.6: Block diagram of OFDM-NOMA

shift sequence (CSS) PTS. In [63], different unitary transforms, such as WHT, ZCT, and the discrete Hartley transform, are employed by Arsla Khan et. al., to minimize the occurrence of high peaks. Furthermore, in [63], the authors have used T-transform, a mix of WHT and ZCT, as a new pre-coding strategy to tackle the problem of high PAPR in OFDM-based NOMA systems. Herein, we propose Trellis Shaping to overcome the problem of high PAPR in NOMA-OFDM systems.

Chapter 3

PAPR Reduction Techniques, A Literature review

3.1 Performance Analysis of PAPR of OFDM System

OFDM is now receiving intensive development for wireless transmission due to its endurance against multi-path fading channels. It does, however, has a major flaw, i.e., the high PAPR, which is a main hurdle for the practical application of the OFDM/ multicarrier systems. Efficiency of the system is reduced in case of high PAPR, as the signal is clipped by the non-linear circuitry's. Subsequently, we'll discuss about PAPR, how to quantify PAPR, and the counter-measures taken so far for PAPR reduction.

3.2 PAPR Of OFDM System

3.2.1 Peak-to-Average Power Ratio

OFDM have many advantages including no/minimum ISI, ease in implementation using DFT/ IDFT, have optimal spectrum utilization with the overlapping orthogonal sub-carriers, all of which have led to its adoption in current communication systems. However, the OFDM symbol inherits a key flaw, i.e., it has high PAPR. The symbols modulated with $\mathcal{M} - QAM$ are believed to be dispersed in a uniform manner, i.e., are i.i.d., which results in a Gaussian-like distribution according to the Central Limit Theorem (CLT). As a result, the TD signal's peak power and average power are drastically different. The difference between an OFDM signal's peaks power to its average power is known as PAPR [31], mathematically defined as

$$\text{PAPR}(x) = \frac{\max\limits_{1 \leq k \leq N} [|x_k|^2]}{E\{|x_k|^2\}} \ , \tag{3.1}$$

where $\max|x_k|^2$ represents peak power of the envelope and $E\{|x_k|^2\}$ denotes the average power over an interval $1 \leq k \leq N$ of the OFDM symbol.

3.2.2 PAPR and Crest factor

In literature, both PAPR and crest factor are often used interchangeably, however, both the terms are different from each other. It is a way of decreasing high PAPR of the TD signal such that power amplifier at the transmitter side will be operated efficiently. The crest factor of a waveform is a measurement of how high the peaks are. It is used to calculate the ratio of the peak to effective mean value. Extreme peaks of the waveform are denoted by crest factor. Mathematically, crest factor can be written as

$$C_f(s(t)) = \frac{\max|s(t)|}{\max|s(t)^2|} \tag{3.2}$$

However, squaring the crest factor gives the PAPR, i.e.,

$$PAPR = c_f^2 \qquad \text{or} \qquad C_f = \sqrt{PAPR} \tag{3.3}$$

PAPR and Crest factor are equal when measured in dBs.

3.2.3 Cumulative distribution function (CDF) and Complementary CDF (CCDF)

To evaluate and compare the system performance in terms of PAPR, CCDF is used in the literature to calculate how long a signal stays above its average power limit. It is also used for investigating the PAPR reduction in OFDM systems. It essentially illustrates an OFDM frame's PAPR in contrast to a pre-defined threshold τ. Mathematically:

$$\text{CCDF(PAPR)} = P_r > \tau \ . \tag{3.4}$$

For understanding the statistical analysis, let $X = [x_n]$ be an input of i.i.d. $\mathcal{M} - QAM$ symbols with variance $\sigma_k^2 = [x_k x_k^*]$ and zero mean. The probability density function (pdf)

can then be defined as

$$\text{pdf}(x_k) = 2x_k e^{-|x_k|^2} \tag{3.5}$$

The CDF can then be formulated as

$$CDF(\tau) = CDF_{\tau_k}(\tau) = (1 - e^{-\gamma})^N \ , \tag{3.6}$$

and the CCDF can be obtained as

$$CCDF(\tau) = 1 - CDF_{\tau_k}(\tau) = 1 - (1 - e^{-\gamma})^N \ . \tag{3.7}$$

3.3 Consequences of High PAPR

Compared to a single carrier system, OFDM has the capacity to reliably transmit data at higher rate, however, the main disadvantage of OFDM is its high PAPR. The transmit signal in time domain has huge dynamic range, i.e., it has infrequent peaks that are higher than the average power of the signal. These peak excursions drives the power amplifier to operate in non-linear region, leading to signal clippings which in turns results in signal distortion and spectral spreading. Occurrence of high peaks in a signal envelop takes place whenever numerous signals' instantaneous amplitudes have high peaks aligned at the same moment. Many electronic devices (such as: A/D converters, HPA) have power limitations (for high peak power). Thus, signal's having high peaks when passes through these non-linear devices get clipped. When the signal is clipped, it will cause disruption in the signal, which will affect the system's performance and it will degrade the performance in terms of BER. Actions must be taken to alleviate high PAPR.

The solution to tackle this problem is, we can use high power back-offs with the non-linear devices. Another solution is to operate HPA with high power backs, however, it is inefficient in terms of power efficiency. Before passing the signal through non-linear devices, alternative steps must be taken to limit these peak excursions. Many algorithms have already

been proposed in the literature to solve this problem. Some of the well known approaches proposed for SISO-OFDM are discussed subsequently.

3.4 PAPR Reduction in SISO-OFDM systems

Many methods for lowering PAPR have already been suggested in the literature which can be divided into three categories, i.e., signal distortion methods, multiple signaling and probability methods, and coding techniques.

3.4.1 Signal distortion techniques

The main idea is to distort the signal before transmitting it through the PA, by doing so we can reduce PAPR. This technique is further divided into four other PAPR reducing techniques, as mentioned below.

Clipping and filtering

In clipping [], before passing a signal through the HPA, the high peaks of an OFDM signal are clipped. This method uses a clipper to limit the signal to a predetermined clipping level; if the signal exceeds the limit τ, the clipper will clip the signal; otherwise, the signal will pass through, unaltered [40]. Mathematically, amplitude clipping can be defined as

$$\mathbf{C}(x) = \begin{cases} x, & |x| \leq \tau \\ A, & |x| > \tau \end{cases}, \tag{3.8}$$

where τ denotes the clipping level, which has been set to a positive number. Non-linear processing is required to avoid clipping. Clipping is a non-linear method resulting in-band distortion and out-of-band radiation. This will affect the BER and spectral performance of an OFDM system. Filtering is applied to eliminate the out-of-band disruption, however, it does not help in eliminating the in-band disruption. This will result in peak re-growth, however, the BER is improved. The in-band distortion can be eliminated by taking multiple FFt's/IFFT's, which increases the computational complexity.

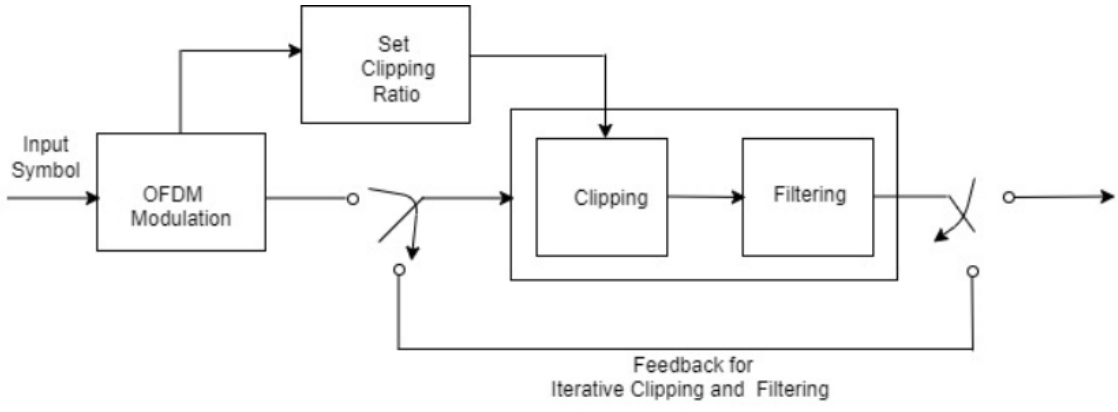

Figure 3.1: Clipping Model

Peak Windowing

In peak windowing [], the high peaks can be restricted by multiplying a weighting function known as windowing function with the higher peaks of the signal. Commonly used windowing function in the literature are Hamming [], Hanning [], and Kaiser []. By matching the window function with signal samples in such a way that its valley is amplified by the signal's peaks, the PAPR is lowered. The higher amplitudes of the signal samples get multiplied with the lower amplitude of the signal's samples. As compared to clipping, it will smooth out the signal in a better way resulting in higher reduction in PAPR.

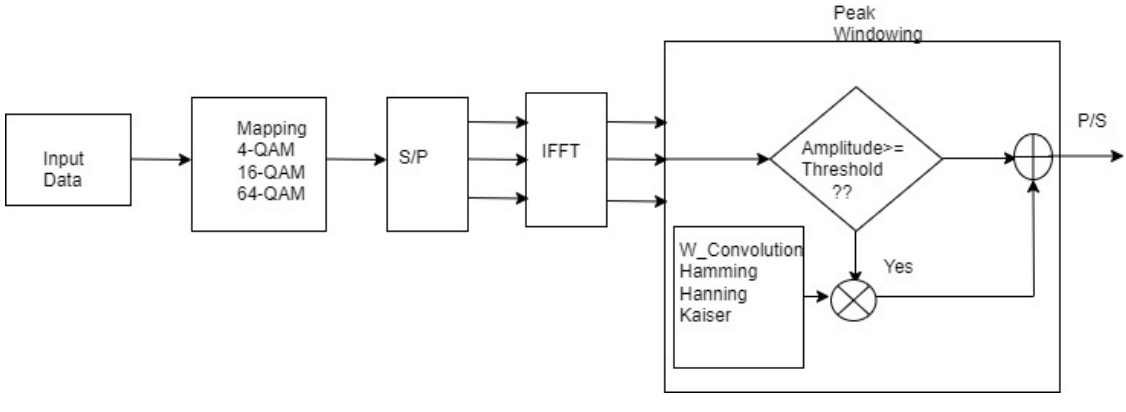

Figure 3.2: Peak Windowing Model

Companding

Companding is typically used for voice signals, however, it can also be used for OFDM signals to reduce PAPR as the peaks occur seldom. Companding has less complexity than other approaches, moreover, its complexity does not alter as the number of sub-carriers increases. LST, LAST, NLST, and NLAST are the four major classes of companding. μ-law companding is another PAPR reduction approach. High peaks are kept while low amplitude signals are increased in μ-law companding. The peak power is maintained but the average power is increased, resulting in a PAPR reduction. After distortion, the companded signals are represented by:

$$x_c[x] = A\frac{log(1+\mu(\frac{|x[n]|}{A})}{log(1+\mu)}\text{sgn}(x[n]) \ , \tag{3.9}$$

where A is the normalization constant and μ is the companding parameter. Before demodulation, the retrieved signal is extended using the equation.

$$x_e[x] = A\frac{e[\frac{x[n]}{A\ \text{sgn}(x[n])}log(1+\mu)] - 1}{\mu\text{sgn}(x[n])} \tag{3.10}$$

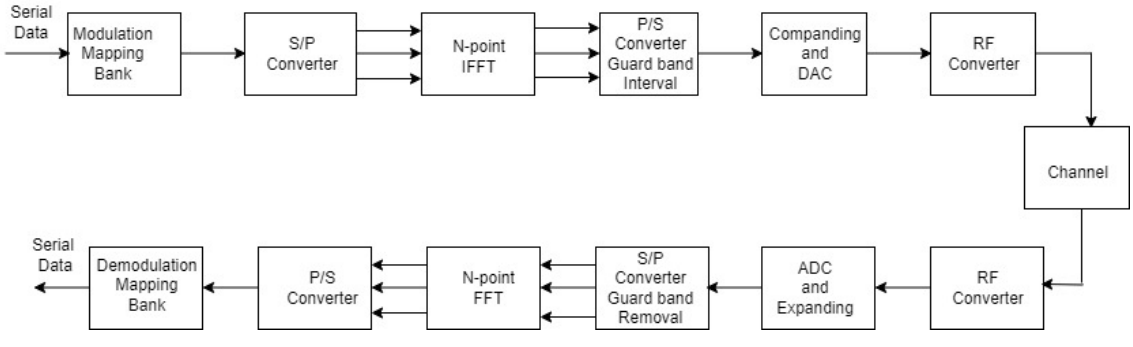

Figure 3.3: Companding Block Diagram

Peak Cancellation

In this technique , multiple waveforms are generated by performing different operations on them, i.e., scaling, shifting, and subtraction to get an appropriate waveform. As the

name indicates, peak cancellation, so it is performing cancellation by subtracting the peak cancellation waveform from the OFDM signal having high peaks. The waveform generated is band-limited to a set of peak cancellation tones that are not used for data transmission.

In OFDM, this technique takes place after IFFT. Peak cancellation can be performed by eliminating the peak cancellation waveform from the OFDM signal whenever the amplitude of the peak exceeds certain threshold. Measure should be taken to avoid the creation of new peaks during this process.

3.4.2 Probabilistic and Multiple Signaling Techniques

This method is beneficial in two ways. The first generates a variety of OFDM signal combinations and sends the one with the lowest PAPR. Altering the OFDM signal by including phase angles, adding peak reduction carriers, or changing the constellation points is the second method. PAPR reduces by optimizing the adjustment parameters.

Selective Mapping

In SLM approach [], multiple OFDM symbols are generated denoted as $\mathbf{X}^m$, $0 \leq m \leq M-1$, each of the symbol is of same length denoted as N. These symbols contain the same data as the original OFDM symbol $\mathbf{X}$. This OFDM symbol set is obtained by multiplying each element of the original data block $\mathbf{X} = [X_1, X_2, \cdots, X_N]$ with each element of the different phase sequences $\mathbf{p}^m$, each having length N and it is represented as

$$\mathbf{p}^m = [e^{j\phi_{m,1}}, e^{j\phi_{m,2}}, \cdots, e^{j\phi_{m,N}}] \qquad 0 \leq m \leq M-1 \tag{3.11}$$

$\phi_{m,k} \in (0, 2\pi]$ for $k = 1, 2, \cdots, N$. The modified symbol $\mathbf{X}^m$ after multiplying element-wise with the mth phase sequence is passed through the IFFT block and transmit the one with the lowest value of PAPR.

SLM's potential to lower the PAPR is driven by two factors,

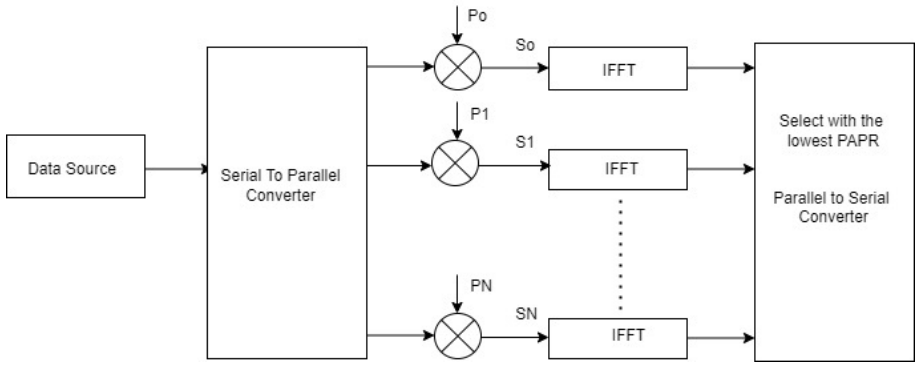

Figure 3.4: Selective Mapping Block Diagram

1. The total number of phase variables

2. Design of phase sequences; However, as the number of phase sequences grows, the system's complexity grows as well, because of this SLM has the disadvantage that it cannot be used in OFDM system with several carriers.

Partial Transmit Sequence

The idea of PTS is similar to that of SLM, however, in this technique is an N-symbol input data set is divided into D disjoint sub-blocks. All of the sub-carriers are adjusted by a phase factor specific to that sub-block. The phase factor chosen has a direct impact on the minimization of the PAPR of the combined signals belonging to any sub block. Each block is N/D in size and is assigned a set of tones, with all other tones set to zero. The PTS block diagram is depicted in Fig. 3.5. The figure shows that the input data block is mapped prior to serial-to-parallel conversion. This entire data set is then divided into sub-blocks and IDFT is performed on each of these blocks. Before transmission, the disjoint signals are combined after all of the sub-blocks have been optimized. The phase factor chosen for rotation affect the PAPR of the combined signal, so it must be chosen carefully. Finally, the sub-block with the lowest PAPR is chosen for transmission. PTS outperforms SLM in terms of performance, but its computational complexity is higher. Aside from that, PTS uses differential coding or must send side-information about the phase-factor.

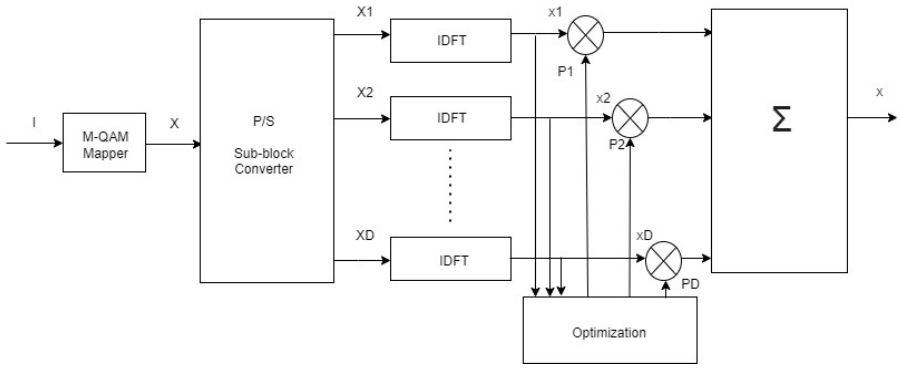

Figure 3.5: Block Diagram of Partial Transmit Sequence

PTS solution:

- Looking for a combination of the sub-blocks with tminimum PAPR involves high processing which, therefore, makes computationally complex.
- Moreover, the ideal phase factors overhead must be supplied to the receiver in order for the transmitted bit sequence to be successfully decoded.

Tone Reservation

The TR algorithm was proposed by Tellado in [31, 32]. The core idea of this technique is that a subset of tones is reserved for reducing PAPR. These tones have low SNR, that's why they are not used to carry any information. The existing tones in an OFDM frame are divided into two sets. One set of tones $\mathbf{X}$ is used to transmit data and the second set $\mathbf{C}$, on the other hand, is reserved for PAPR reduction with $\mathbf{X} \bigcap \mathbf{C} = \Phi$. The reserved set of tones are used to generate a corrective function. Both $\mathbf{X}$ and $\mathbf{C}$ are transformed into time domain using the IFFT modulator to get $\mathbf{x}$ and $\mathbf{c}$, where $\mathbf{c}$ is the corrective function in time domain. The corrective function $\mathbf{c}$ is then iteratively added to the transmit signal iteratively for PAPR reduction, mathematically,

$$\tilde{\mathbf{x}} = \mathbf{x} + \mathbf{c} = \text{IFFT}(\mathbf{X} + C) \ . \tag{3.12}$$

The Tone Reservation (TR) algorithm has the following main steps:

- The information vector $\mathbf{X}$ is initialized and the reserved tones are set to 0
- $\mathbf{X}$ is transformed into time domain by taking its IFFT
- The position d of the peak is identified
- If $|x_d|$ is less than the pre-defined threshold τ, the process is terminated. Otherwise,
- The signal is modified before transmission according to:

$$\mathbf{x}^{(i+1)} = \mathbf{x}^{(i)} - \alpha(\mathbf{x}_d^{(i)} - e^{jarg\{\mathbf{x}_d^{(i)}\}} \cdot \tau)(\boldsymbol{r}(N-m)(mod-N) \tag{3.13}$$

The filter response was not taken into account by the TR algorithm given by the authors in [31, 32]. Major drawbacks of TR algorithm are

- Capacity loss due to the reserved tones
- Mean power increase due to the addition of a corrective function with the transmit signal for PAPR reduction.

Tone Injection

In Tone Injection (TI) [], the constellation point in the complex plane is mapped onto multiple outer points, extending the constellation size, i.e., this technique extends the constellation to a higher order constellation. The energy and phase of the constellation point changes when it is mapped to any of the expanded constellation points. The distance between the extended point and the origin determines the symbol's energy in the constellation.

Major drawbacks of the TI algorithm is that due to the combination of signals with the same phase, sometimes, there is a significant increase in PAPR problem. One can adjust the PAPR by changing the phase and lowering the energy of the symbol points. Moreover, In OFDM, a symbol is mapped onto the sub-carrier, which is nothing more than a frequency

or a tone. When you increase the power of a symbol, you are injecting a tone, which means you are giving more power to that symbol or injecting a tone to make it to a higher order constellation, and you are also increasing the energy. Noise will arise if the distance between the original constellation point and the extended constellation point is too near, affecting detection. The following condition must be met in order to maintain the spacing between the points, i.e.,

$$D = \delta d\sqrt{M} \tag{3.14}$$

Advantage of this technique is that it does not require any side information to be sent along with the OFDM signal.Drawback is that the OFDM signal's average power will increase. Moreover, an optimizer is required to pick the optimum points on which the original constellation point must be mapped which, thus, increases the computational complexity at the transmitter.

Active Constellation Extension

Active constellation extension (ACE) was first proposed by D.L Jones in [48]. The author suggested a method termed as active channel modification for PAPR reduction in OFDM and discrete multi-tones. In active constellation method, the outer constellation points in the mother constellation are extended outwards and after that convex optimization is used to identify the set of the extended points that best reduces the PAPR of the transmit signal. Moreover, beside PAPR reduction, ACE has the capability to reduce the BER as well. A major drawback of ACE is that it is computationally demanding. Afterward, S. Krongold and G.R Wood [49,50] suggested a modified algorithm that improved the results of OFDM's PAPR reduction with the help of ACE. The suggested method is really efficient, but it is also computationally demanding as the process involves convex optimization. Besides that, there is an increase in the mean transmit power due to constellation extension.

Trellis Shaping

Initially, G.D Forney suggested the idea of Trellis shaping for reducing the average power [34]. Henkel and Wagner were the one who suggested the concept of using Trellis Shaping for PAPR reduction in multi-tone systems for the first time in [35], with further extensions in [36,37,38,39]. The author proposed two metrics, the first metric is in time-domain and the second one is in frequency domain, as a branch metric for trellis shaping codes [36]. It was found that the time domain metric performance is better than the frequency domain metric, however, it has higher computational complexity because of using various DFT/IDFT pairs. TS is widely recognized as the most adaptable and appropriate PAPR reduction technique in literature. Trellis shaping needs no side information transmission and is easily applicable in almost all systems. Trellis shaping, unlike other PAPR reduction techniques, does not introduce any nonlinear deformations. For the application of TS for PAPR reduction, a technique with minimum complexity was developed that used autocorrelation of the side lobes of the transmit signals in frequency domain by Ochiai in [45]. Trellis shaping performs constellation shaping like coded modulation but does not provide any error correction which shows that it relatively has a lower noise margin. Our work is based on PAPR reduction using Trellis Shaping so we will discuss it in details in the next chapter.

3.5 PAPR reduction in OFDM-NOMA

A lot of PAPR reduction techniques have been proposed in the literature for conventional OFDM systems as discussed earlier. So far very few PAPR reduction techniques have been proposed for OFDM-NOMA system. Here we will be discussing those techniques in detail

3.5.1 Precoding Method

Arsla Khan proposed this method for the first time for PAPR reduction in the OFDM-based NOMA system [17]. PAPR is reduced by multiplying the input data sequence with differ-

ent precoding matrices such as Walsh Hadamard Transform matrix, Zadoff Chu Transform matrix, T-transform matrix, Discrete Fourier transform, Discrete sine matrix transform, Discrete cosine matrix transform and Discrete hartley matrix transform . After multiplying the modulated input data sequence with any of these matrices the resultant signal vector will be passed through an IFFT block as shown in the given block diagram. Consider 1 × N modulated input data vector of the ith user as $\boldsymbol{X^{(i)}} = [X_0^{(i)}, X_1^{(i)}, ..., X_{N-1}^{(i)}]$ If we have a N × N precoding matrix and call it $\boldsymbol{P}$, then 1 × N precoded input data vector for the ith user will be mathematically represented as:

$$\boldsymbol{D}^{(i)} = \boldsymbol{X^{(i)}}\boldsymbol{P} = [D_0^{(i)}, D_1^{(i)}, ..., D_{N-1}^{(i)}] \tag{3.15}$$

$P_{i,m}$ is the precoding matrix element in mth row and nth column where $0 \leq i, m \leq N-1$ At the receiver end the recieved signal gets multiplied with the inverse precoding matrix to decode the recieved data. Mathematically represented as:

$$\tilde{\mathbf{X}}^{(i)} = \tilde{\mathbf{D}}^{(i)}\boldsymbol{P^{-1}} = [\tilde{\mathbf{X}}_0^{(i)}, \tilde{\mathbf{X}}_1^{(i)}, ..., \tilde{\mathbf{X}}_{N-1}^{(i)}] \tag{3.16}$$

Where $\tilde{\mathbf{D}}^{(i)}$ is the recieved signal of the ith user after SIC and $\boldsymbol{P^{-1}}$ is the inverse precoding matrix This method doesnot need side information to be transmitted and therefore doesnot degrade the performance of the system in terms of BER. This method's PAPR reduction property is inferior to that of PTS-based methods.

3.5.2 Dummy Sequence Insertion Method

It is another PAPR reduction method implemented in OFDM-NOMA system [62]. In this method the input data sequence is combined with a dummy sequence to generate first candidate signal and later passes through an IFFT block if its PAPR value is less than the given threshold the system transmits the signal otherwise another dummy sequence is generated

and added to the input data sequence and generates the second signal and pass it through the IFFT block and the system will recheck the PAPR value. This process will be continued until we find an appropriate signal whose PAPR value is less than the given threshold. If there is no such signal, then we will transmit that signal who has the least PAPR value. The dummy sequence symbols contain no information so they can be ignored easily at the reciever end and there will be no data loss. In this method there is no need to transmit side information, therefore there will be no degradation in the performance of the system in terms of BER. It has a low PAPR reduction property as compared to the other technique, and it is computationally complex

3.5.3 PTS-based Method

Three different PTS-based methods are proposed in the literature for OFDM- NOMA system, they are:

- C-PTS Method [62]
- DSI-PTS Method [**?**]
- DSI- Cyclic Shift Sequence PTS Method [?]

C-PTS Method

Here the block of input data symbols is divided into M-disjoint sub-blocks using the Interleave (IL-PTS), Adjacent (AP-PTS), or Pseudo-Random (PR-PTS) partitioning schemes. After partitioning the each subblock passes through an IFFT block and each symbol gets multiplied by a phase rotation factor b_m. Then each disjoint sub-block recombine to get first signal. The system takes the phase rotation factors from the following set of vector:

$$b_m \in \{e^{\frac{j2\pi v}{V}} | v = 0, 1, ..., V-1\} \tag{3.17}$$

b_m is the phase rotation vector, V is the number of possible phases of rotation vector. After multiplying each of the M sub-block with V different phases of the rotation vector and combining them, the system will transmit the signal having least PAPR value. This system has

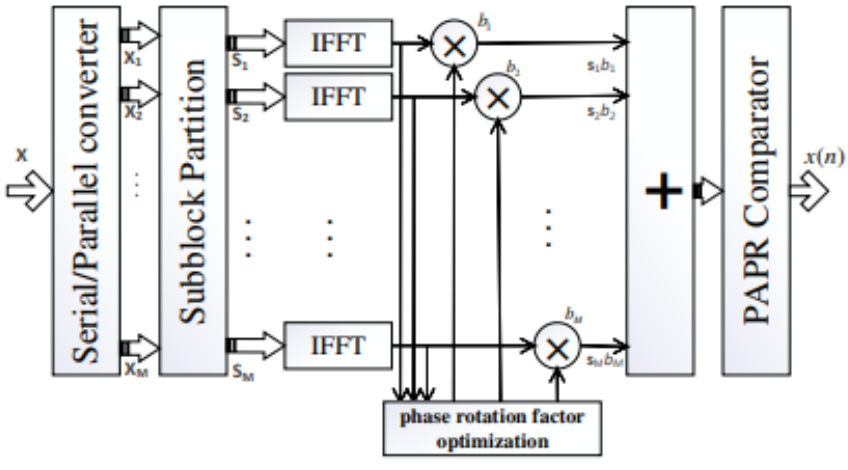

Figure 3.6: Block Diagram of C-PTS Method

a high PAPR reduction property, but it has an advantage that it must send the information of the selected phase rotation factors to the receiver, this reduces the BER performance of the receiver. Moreover, the main disadvantage of PTS-based methods is their high computational difficulty.

DSI-PTS Method

As shown by the block diagram, the DSI-PTS method inserts a dummy sequence into the input data sequence. The new input block is made up of K data symbols and L dummy symbols, as shown by W, where L = K and L+K = N. Later, the input data symbol block is divided into M disjoint subblocks. The IFFT block is then used to transform each subblock from the frequency domain to the time domain. Then, for each time-domain subblock s_m, a phase rotation factor b_m is multiplied. The phase rotation vector is represented as:

$$b_m \in \{e^{\frac{j2\pi v}{V}} | v = 0, 1, ..., V-1\} \tag{3.18}$$

After multiplying each of the M sub-block with V different phases of the rotation vector and recombining them we get the first group of signals . The signal with the lowest PAPR value is chosen as the first candidate signal after constructing the first group of signals. The signal will be transmitted if its PAPR value is less than the threshold. Otherwise, a new dummy sequence is inserted, and the previously described process is repeated. This process is repeated until all possible candidate signals are identified. If no signals with PAPR values less than the threshold are found, the signal with the lowest PAPR value is chosen to be transmitted. The computational complexity of the DSI-PTS method remains

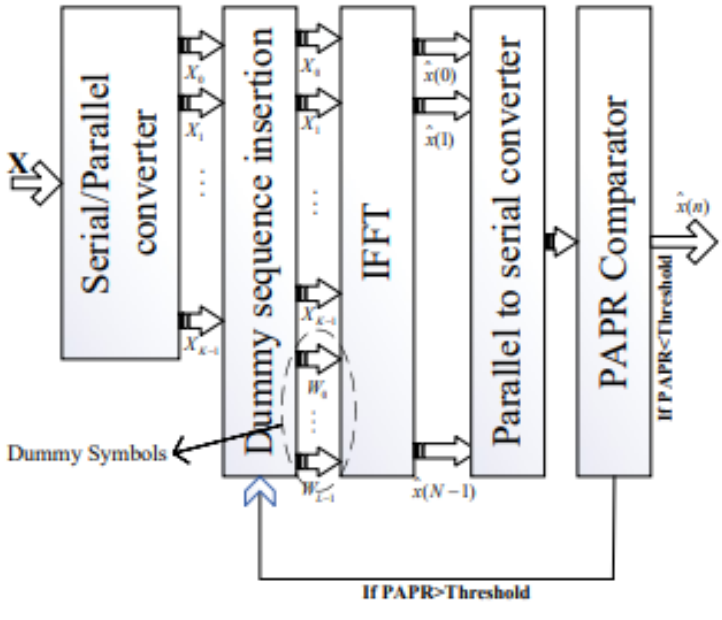

Figure 3.7: Block Diagram of DSI-PTS Method

high. In addition, in this method, the transmitter must send the chosen phase rotation factors to the receiver in order for it to decode the transmitted data. As a result, this method degrades the system's BER performance.

DSI-Cyclic Shift Sequence PTS Method

After inserting the first dummy sequence into the input block and dividing it into subblocks, each subblock is passed through the IFFT operator in this method. Instead of multiplying

the disjoint subblocks by the phase rotation factors, new candidate signals are generated by cyclically shifting and recombining the subblocks in the time domain. Similarly to the DSI-PTS method, the system will check the PAPR value in each iteration until it finds a proper signal with a PAPR value less than or equal to the threshold. As previously stated, C-PTS and DSI-PTS methods require a large number of operations to generate candidate signals, whereas DSI-CSS requires far fewer. Furthermore, the DSI-CSS method reduces PAPR slightly better than the DSI-PTS and PTS methods. It does not require the transmission of side information, which is required for detecting the transmitted data in the C-PTS and DSI-PTS methods.

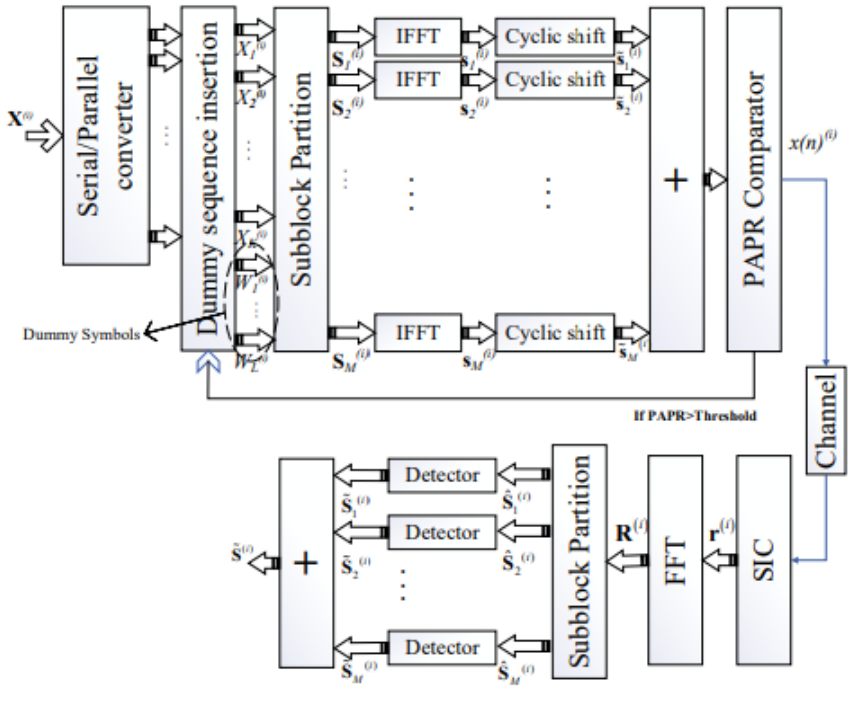

Figure 3.8: Block Diagram of DSI-CSS Method

Chapter 4

TS based PAPR reduction in OFDM-NOMA systems

NOMA is one of the best candidates to fulfill the ever growing demand of mobile traffic. NOMA-based OFDM systems will offer massive connectivity with reliable transmission for multicarrier transmission. However, a major drawback inherited by NOMA-OFDM is its high PAPR which is a big hurdle for future technologies to adapt it. As we know that, due to high PAPR, traditional NOMA are spectral and energy inefficient. Herein, we propose TS as a possible solution to alleviate the problem of high PAPR in down-link PD NOMA-OFDM. Moreover, to further improve the system performance, we will be using shaping codes of different trellis depth in the TS.

4.1 System Model

Herein, we consider a downlink PD NOMA-OFDM system, with two users as shown in Fig. 4.1. Moreover, The BS is considered to be equipped with single antenna feeding two users which are equipped with single antenna as well. As shown in Fig. 4.1, we have two receivers UE_1 and UE_2. Moreover, we consider that UE_2 is far from the BS and is having a bad channel as compared to UE_1 which lie close to the BS. Based on their distances from the BS, UE_2 is assigned more power P_2 as compared to UE_1, such that $P_T = P_1 + P_2$. After $\mathcal{M}$-QAM mapping and power allocation, superposition coding is performed at the transmitter to multiplex the signal of the user by taking advantage in their channel condition. We have to improve the SE of the system. This is possible if certain criteria are met. At the moment, SIC is being performed on the receiver side to extract appropriate data from the superposed signals.

4.1.1 Description

As shown in Fig. 4.1, we have a BS and 2 users each user is transmitting binary data in the form of 0's and 1's. The bits form $\mathcal{M}$-QAM and each symbol is modulated when it is passed through a modulation block where bits are mapped on the constellation points. The $\mathcal{M}$-QAM are then passed through a Trellis shaper, for shaping the symbols to lower down its PAPR. The shaping can be done at two points; before the superposition, where the shaping is performed on individual user. However, doing so will be spectrally inefficient as in that case 2 bits one per each user will be added as redundant bit. An alternative solution will be to apply trellis shaping after superpostion is performed. However, in doing so, the shaping is performed on one user and the data of the other user is provided to the trellis shaper in the matric calculation such that the over all PAPR is minimized. Therefore, to save system's capacity, we are applying TS on one user and pass the other's user data through the modulator as it is. By doing this, we can save capacity one bit per NOMA symbol, however, as a trade-off the PAPR reduction capability is less of this approach. After TS, the NOMA symbols are assigned different power levels to each user as discussed earlier that power is allocated on the basis of the distance between user and the BS. As we are considering PD NOMA-based OFDM system for downlink, so we are allocating more power to the user which is far from the BS and least power to the user which is close to the BS. Lets UE_1 be in a close proximity of the BS, thus we will be assigning less power to UE_1 as compared to UE_2 . The channel condition for UE_1 is better as compared to UE_2. After the allotment of power to the users both the signals of the users are combined together and perform superposition coding. After that the combined signal, i.e., PD-NOMA symbols is passed through a S/P converter. After S/P, the NOMA-symbole are passed through an IFFT modulator and the signal is converted into time domain. To cancel the effect of ISI, a guard band interval CP is added to the time

domain signal and is transmitted through an AWGN channel after P/S converter, where noise is added in the channel.

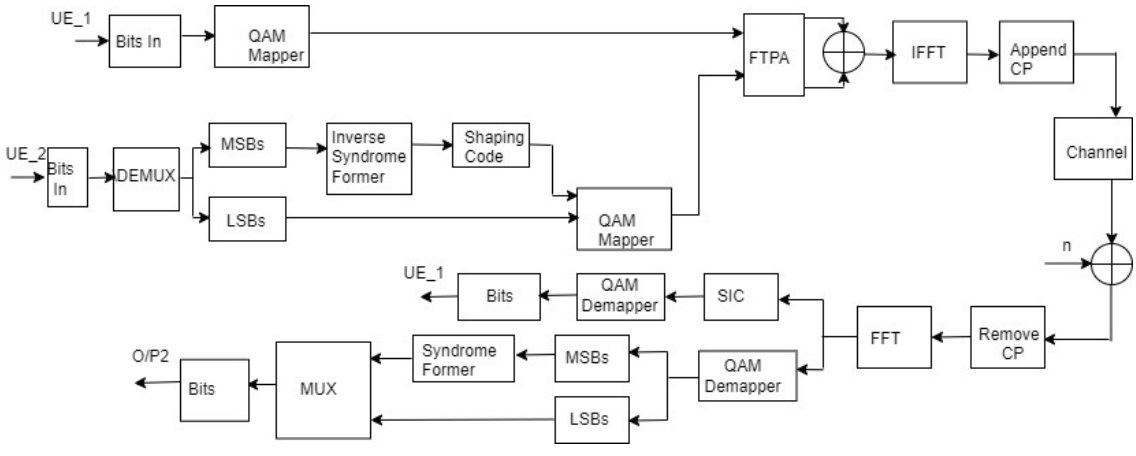

Figure 4.1: Proposed Model

At the receiver, the guard-band interval CP is removed from the received signal. After removing the guard-band, the signal is passed through a S/P converter and an FFT demodulator is used to transform the back into frequency domain. After FFT modulator, the signal is P/S converted. Uptil now all the operations performed on both the users are the same. To recover the individual users data SIC is performed. As both the user's channel condition is distinct from each other thus the recognition method is applied differently. As we know that UE_1 has allocated least power, therefore, to recover the signal of UE_1 SIC is applied on the received NOMA signal. Here the UE_1 is containing residual of UE_2 as interference. For UE_1, the strongest signal having more power is subtracted from the received signal and to get the signal of UE_1. A QAM-demodulator is later on used to demap the desired data of UE_1 . Moreover, UE_2 is the strongest signal so it will pass as it is to the QAM-demodulator and will be demapped for the desired data of UE_2

4.2 Trellis shaping for PAPR reduction in NOAM-OFDM

Trellis shaping is the most promising techniques used to limit the high PAPR. For limiting the PAPR, we propose trellis shaping for PAPR reduction in NOMA-OFDM systems. Moreover,

as a metric for search in the trellis of shaping code, the auto-correlation of the side-lobes of an OFDM signal is considered over here as proposed by Ochiai []. Moreover, we will be considering the Type-I modullation as proposed by Ochiai.

4.2.1 TS System Model

Figure 4.2 shows block diagram of Trellis shaping, where C_s is the shaping code with rate k/n where k is the total input bits to the encoder and n is the output bits. Let's $\mathbf{G}$ be the generator matrix of the convolutional shaping code C_s. The shaping code that is mostly used is rate $1/n_s$, where n_s is the number of the output bits. Let $\mathbf{G}$ be $1 \times n_s$ generator matrix of the shaping code and let $\mathbf{H}^T$ represents $n_s \times (n_s - 1)$ parity check matrix and $(\mathbf{H}^{-1})^T$ represents $(n_s - 1) \times n_s$ left inverse syndrome former of the shaping code. In our work, we have employed a rate $\frac{1}{2}$ convolutional codes as our shaping code. Let $\mathbf{u}$ be the input bit sequence used for transmission having length $1 \times (B-1)N$, where $B = log_2(M)$, $\mathcal{M}$ is the size of the constellation and N is the OFDM frame size. The input bits are demultiplexed into two bits streams, i,e., '$\boldsymbol{m}$' and '$\boldsymbol{n}$' as shown in the figure. $\boldsymbol{m}$ is referred as MSBs and

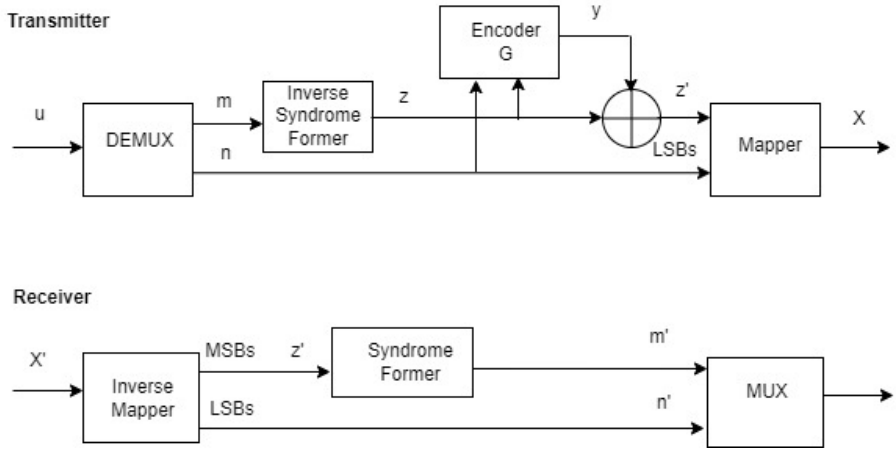

Figure 4.2: Block Diagram of Trellis Shaping

$\boldsymbol{n}$ is referred as LSBs. The MSBs are first encoded by passing them through the inverse

syndrome former, $(\mathbf{H}^{-1})^T$ and we will get $\boldsymbol{z}$ on the output represented as:

$$\mathbf{z} = \mathbf{m}(\mathbf{H}^{-1})^T \tag{4.1}$$

The LSBs are passed as it is. The generated output sequence $\boldsymbol{z}$ is modulo-2 added with a valid code sequence $\boldsymbol{y}$ from the shaping code $\boldsymbol{C_s}$ and we will get $\boldsymbol{z}^{'}$ i.e.,

$$\mathbf{z}^{'} = \mathbf{z} \oplus \mathbf{y} \tag{4.2}$$

where

$$\mathbf{y} = \mathbf{iG} \tag{4.3}$$

$\mathbf{G}$ is the Generator matrix, and $\mathbf{i}$ is an arbitrary input bit sequence such that $\mathbf{GH}^T = \mathbf{0}$, where $\mathbf{0}$ is an all zero vector of size $1 \times (n-k)$.

In order to get the information encoded at the transmitter by the inverse syndrome former $(\mathbf{H}^{-1})^T$, the sequence $\mathbf{y}$ is right multiplied by $\mathbf{H}^T$, i.e.,

$$\mathbf{yH}^T = 0 \tag{4.4}$$

whereas $\mathbf{y}$ is said to be a valid code sequence in $\boldsymbol{C_s}$.

To retrieve the input data set $\mathbf{m}$ at the receiver side, $\mathbf{z}^{'}$ is passed through the parity check matrix $\mathbf{H}^T$ as:

$$\mathbf{z'H}^T = \mathbf{z} \oplus \mathbf{yH}^T = \boldsymbol{zH^T} \oplus \underbrace{\mathbf{yH}^T}_{=0} \tag{4.5}$$

$$\boldsymbol{z'H^T} = \boldsymbol{zH^T} \oplus \mathbf{0} = \boldsymbol{m}\underbrace{(\boldsymbol{H^{-1}})^{\boldsymbol{T}}\boldsymbol{H^T}}_{=I}$$

$$\boldsymbol{z'H^T} = \boldsymbol{mI} = \boldsymbol{m}$$

4.2.2 Sign-bit Shaping

Sign bit shaping begins with a square constellation such as 16×16 square constellation. Each coordinate of this constellation takes up values from the 16-point PAM constellation,

i.e., $\pm\frac{1}{2}, \pm\frac{3}{2}, \cdots, \pm\frac{15}{2}$ and is normalized such that the minimum distance between the constellation points d_{min} is 1. In two's complement notation, the value of each coordinate is represented by "$zabc$". In this case, z is the most significant bit. The remaining bits abc are designated as the least significant bits. Each 2-bit output of the shaping code is used as an MSB, which selects one of the $\mathcal{M}$-QAM constellation's in the four quadrants [45]. Furthermore, we consider Gray mapping for the $\mathcal{M}$-QAM constellation known as Type-1.

4.2.3 Constellation Mapping for Sign-bit Shaping

Herein, we consider a rate $1/2$ convolutional code for the sign bit shaping as in [47]. $(\mathbf{H}^{-1})^T$ encodes the msbs $\mathbf{m}$ data sequence to produce the binary sequence $\mathbf{z}_k$, where $\mathbf{z}_k$ has a well-established codeword $\mathbf{y}$. The msb is used to select a quadrant from the $\mathcal{M}$-QAM constellation because $\mathbf{z}_k$ and $\mathbf{y}_k$ are both binary. For the LSBs, we will consider Type-1 mapping. The four points in the equivalent class form uniformity with respect to both axes in Type-1 mapping. Because msbs selects the same energy points, this mapping does not possesses the capability to reduce average power, which thus makes it ideal for the PAPR reduction. The results in [33] shows that Type-1 mapping gives substantial PAPR reduction.

4.2.4 Metric Selection for PAPR Reduction in NOMA-OFDM

The metric calculation strategy for the shaping decoder used for PAPR reduction in trellis shaping is critical. Various metrics for the Viterbi algorithm have been proposed in the literature. These metrics exist in both the time and DFT domains. Positive and additive branch metrics are required for valid branch metrics [44]. In [41], the peak power of the transmit signal was chosen as the branch metric (time domain) for finding a valid code sequence in the shaping code Cs. However, because peak power is not additive, this metric does not meet the requirements of a branch metric. This metric directly applies the PAR

criterion to the code sequence. The T.D peak power is calculated and updated at each path.

$$x_{kv} = x_{kv-1} + \sum_{n=(v-1)l+1}^{vl} X_n e^{j}\left(\frac{2\pi}{N}\right)kn \tag{4.6}$$

This branch metric produces excellent outcomes, but it has a drawback that it has high computational complexity. In the DFT domain, [41] suggested an alternative branch metric that was highly dependent on the phase of the symbols and the tabulation of the block transition matrix. This method, however, was limited to small block sizes. Another branch metric proposed for papr reduction in the Viterbi algorithm takes non - continuous auto correlation of the side lobes of OFDM signals into account. Mathematically represented as:

$$\lambda(y_k) = \sum_{m=1}^{kn_s} |\rho| \tag{4.7}$$

This branch metric is used to find a valid code sequence Cs. Another branch metric is suggested by Ochiai in which author minimizes the sum of square of auto-correlation function $\sum_{m=1}^{n-1} |\rho|^2$ is applied to reduce PAPR. Because this metric is additive, it gets priority over the previous branch metric, which only uses auto correlation of the side lobes.

$$\lambda(y_k) = \sum_{m=1}^{kn_s} |\rho|^2 \tag{4.8}$$

Autocorrelation Representation of the OFDM Signal

Now, a metric that can be used in conjunction with the viterbi algorithm to minimize the auto correlation of OFDM sequence side lobes is presented in [33]. Consider an OFDM signal s(t) with N-subcarriers, which is written as:

$$s(t) = \sum_{t=\infty}^{\infty} s_l(t) g(t - lT_s) \tag{4.9}$$

Here, g(t) is the windowing function and T_s refers to the symbols period. The lth complex base band OFDM symbol $s_l(t)$ centered at zero frequency is given by:

$$s_1(t) = \frac{1}{\sqrt{N}} \sum_{k=0}^{N-1} A_{l,k} e^{\frac{j2\pi(k-\frac{N-1}{2})t}{T_u}} \tag{4.10}$$

Where $A_{l,k}$is the complex modulated symbol after trellis shaping. From the above equation, we get [33]

$$|s_l|(t) = \frac{1}{N} R_0 + \frac{2}{N} \sum_{m=1}^{N-1} |R_m| \cos(2\pi m \frac{t}{T_u} + arg R_m) \tag{4.11}$$

Here, R_m shows the a periodic auto correlation function of the complex OFDM symbol defined for m = 0, 1, ...N 1 as:

$$R_m \triangleq \sum_{k=0}^{N-1-m} A_{k+m} A_k^* \tag{4.12}$$

In the above equation, the first term is the dc component while the remaining term shows the fluctuations in the OFDM symbol envelope [38]

$$y = arg \min_{y \in C_s} \sum_{m=1}^{N} |R_m| \tag{4.13}$$

This helps in the selection of a code word such that the auto correlation of its side lobes is minimized. This aids in reducing the waveform fluctuations hence the dynamic range is reduced.

Metric Design for the Viterbi Algorithm

In this case, a slightly different approach is used, namely to lessen the square of the absolute value of the side lobes, which is mathematically represented as [38]

$$y = arg \min_{y \in C_s} \sum_{m=1}^{N} |R_m|^2 \tag{4.14}$$

It is possible to make this minimization recursive. Assume that each shaping symbol is capable of powering n subcarriers. The shaping symbol y_k is chosen at the k_{th} stage according

to:

$$y_k = arg \min_{y \in C_s^k} \sum_{m=1}^{N} |R_m^i|^2 \tag{4.15}$$

C_s^k is the set of the k_{th} symbols of the shaping code C_s, $\mu^{(i)}$ is defined as:

$$\mu^{(i)} \triangleq \sum_{m=1}^{i-1} |R_m^i|^2 \tag{4.16}$$

Where $R_m^{(i)}$ is the aperiodic auto correlation of length i complex signal. The total number of subcarriers processed up to the k_{th} stage are given by:

$$i = (k+1)n \tag{4.17}$$

Metric for Sign-Bit Shaping

The recursive relationship for sign-bit shaping is as follows

$$R_m^i = R_m^{i-1} + \delta_m^{i-1} \quad \text{i=2,3,.....,N} \quad and \quad m = 1, 2, ...i-1 \tag{4.18}$$

Where

$$\delta_m^{(i)} \triangleq A_i A_{i-m}^* \tag{4.19}$$

To reduce the computational complexity all of the entries of $\delta_m^{(i)}$ can be computed beforehand. By substituting the values in the above equation $\mu^{(i)}$ is represented as:

$$\mu^{(i)} = \mu^{(i-1)} + \sum_{m=1}^{(i-2)} 2R(R_m^{(i-1)*} \delta_m^{(i-1)}) + \sum_{m=1}^{i-1} |\delta_m^{(i-1)}|^2 \tag{4.20}$$

The energy of the sub-carrier symbol is represented by the final element in this equation. For Type-1 mapping, regardless of the path taken, this remains constant, so for mapping techniques where average power reduction is not a concern, this can be omitted. Because it uses a recursive approach, the computational complexity of this metric calculation is higher than that of a typical viterbi decoder.

4.3 Shaping codes with higher trellis depths

For PAPR reduction, shaping codes are utilized to shape the $\mathcal{M}$-QAM constellation. Herein, we also consider shaping codes of different shaping depths as it will further improve the system performance in terms of PAPR. These shaping codes are characterized by their generator matrix $\mathbf{G}$, syndrome former $\mathbf{H}^T$ and their left inverse syndrome former $(\mathbf{H}^{-1})^T$. Herein, we presents the best convoluationl codes available in the literature.

4.3.1 4-State (5,7) Shaping Code

(5, 7) shaping codes have a 4-state trellis, with constraint length $L = 2$ and a minimum hamming distance d_{free} = 3. The encoder has two memory units, or shift registers as shown in Fig. 4.3. The generator matrix for this 4-state shaping code in the D domain can be written as

$$\mathbf{G} = [1 + D^2, 1 + D + D^2] \tag{4.21}$$

The parity check matrix of this shaping code is denoted by $\mathbf{H}^T$ and its inverse syndrome

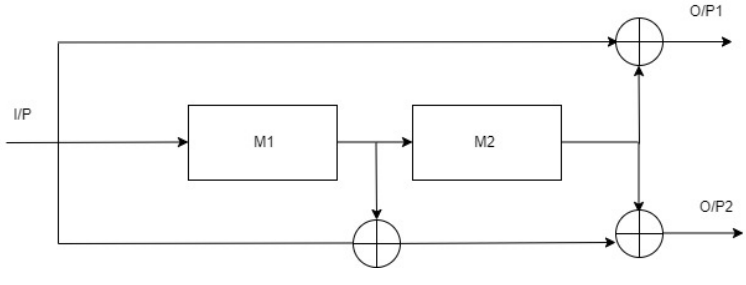

Figure 4.3: Generator Matrix for (5,7) Shaping Code

former matrix is denoted by $(\mathbf{H}^{-1})^T$ at the receiver side. This inverse syndrome former is employed at transmitter side to encode the bit stream which forms the MSBs whereas the LSBs are passed directly without encoding.

The parity check matrix $\mathbf{H}^T$ for the (5, 7) in D-domain is given as:

$$\mathbf{H}^T = [1 + D + D^2, 1 + D^2] \, , \tag{4.22}$$

and its left inverse syndrome former $(\mathbf{H}^{-1})^T$, as shown in Fig. 4.4, is defined in D-domain as

$$(\mathbf{H}^{-1})^T = [D, 1 + D] \tag{4.23}$$

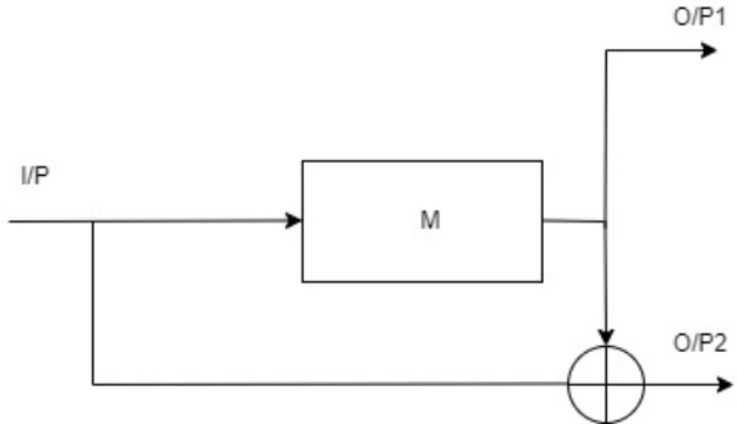

Figure 4.4: Inverse Parity Check Matrix for (5,7)Shaping Code

Bit Error Probability for 4-state Trellis

For the approximation of the bit-error probability of a four state trellis, union bound is used. Union bound is used to find the error probabilities of the bits previously encoded by $(\mathbf{H}^{-1})^T$. The Union bound is based on tree parameters and they are minimum hamming distance d_free, Code's weight distribution A_d and P_{dfree} the likelihood of a wrongly choosen path at distance d. Union bound gives the sum of the error probabilities of the input bit sequence over all paths across distance d.

$$P(E) = \sum_{d}^{\infty} A_d P_{d_{free}} \tag{4.24}$$

Considering an AWGN channel, the probability of choosing an inaccurate path at a distance d is:

$$P_d = \frac{1}{2} erfc(\sqrt{\frac{E_s}{N_0} d_{free}}) \ , \tag{4.25}$$

where $\frac{E_s}{N_0}$ represents signal-to-noise ratio for AWGN channel. The general equation for calculating bit-error probability is represented as:

$$P(b) \approx \frac{1}{k}\frac{1}{2}B_{d_{free}}(e^{\frac{-E_s}{N_0}})^{d_{free}} \tag{4.26}$$

4.3.2 8-State (13,15) Shaping Code

In octal notation, the (15, 17) shaping code corresponds to (13, 15) in decimal notation and creates an 8-state trellis with a constraint length $L = 3$. For this shaping code, the minimum hamming distance d_{free} is 6 where its encoder contains three memory units, as shown in Fig. 4.5. In D-domain, the generator matrix for this 8-state shaping code is given below

$$\mathbf{G} = [1 + D^2 + D^3, 1 + D + D^2 + D^3] \tag{4.27}$$

The parity check matrix is $\mathbf{H}^T$ and its inverse syndrome former matrix is denoted by $(\mathbf{H}^{-1})^T$

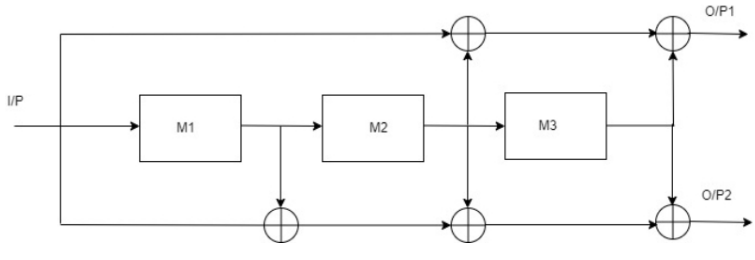

Figure 4.5: Generator Matrix for (13,15) Shaping Code

at the receiver side. This inverse syndrome former is employed to encode the bit stream at transmitter side which forms the MSBs. In D-domain, the syndrome former of (13, 15) $\mathbf{H}^T$ can be written as

$$\mathbf{H}^T = [1 + D + D^2 + D^3, 1 + D^2 + D^3]\ , \tag{4.28}$$

whereas its inverse syndrome former $(\mathbf{H}^{-1})^T$, as shown in Fig. 4.6 is

$$(\mathbf{H}^{-1})^T = [D + D^2, 1 + D + D^2] \tag{4.29}$$

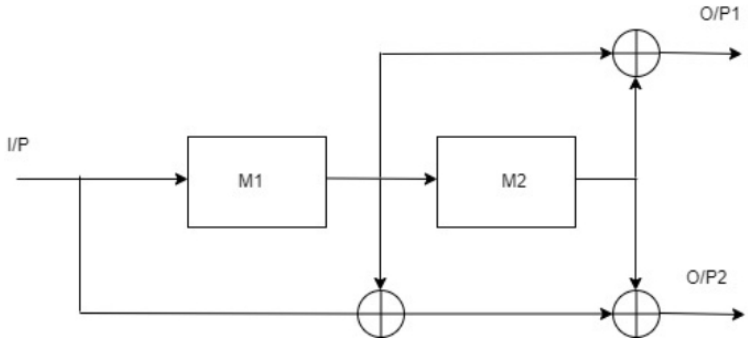

Figure 4.6: Inverse Parity Check Matrix for (13,15) Shaping Code

Bit Error Probability for 8-state Trellis

Same as for a 4-state shaping code, union bound is used to approximate the bit-error probability for an 8 state shaping code. Union bound is used to find the error probabilities of the bits previously encoded by $(\mathbf{H}^{-1})^T$ with minimum hamming distance d_{free}, code's weight distribution A_d and P_{dfree} the likelihood of a wrongly choosen path at distance d_{free}. For the given code d_{free} = 5. Other parameters for the union bound are rate=1/2 code, k=1, $B_{d_{free}}$= 1, and d_free= 5 for an 8-state trellis, the bit-error probability $Pb_{s,f}$ for the encoded bit sequence is given by:

$$Pb_{s,f} \approx \frac{1}{2}(e^{\frac{S}{N}})^5 \tag{4.30}$$

4.3.3 16-State (19,29) Shaping Code

As shown in Fig. 4.7, the $(23, 35)_8$ shaping code corresponds to (19, 29) in decimal notation and have 16-state trellis. For this shaping code, the minimum hamming distance d_{free} is 7. The encoder contains four memory units. Generator matrix for this 16-state shaping code is given below:

$$\mathbf{G} = [1 + D + D^4, 1 + D^2 + D^3 + D^4] \tag{4.31}$$

The parity matrix $\mathbf{H}^T$ for (19, 29) is given as:

$$\mathbf{H}^T = [1 + D^2 + D^3 + D^4, 1 + D + D^4] \,, \tag{4.32}$$

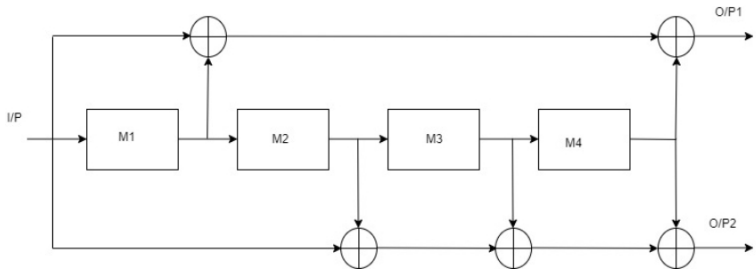

Figure 4.7: Generator Matrix for (19,29) Shaping Code

and its left inverse $(\mathbf{H}^{-1})^T$, as shown in Fig. 4.8, can be defined as

$$(\mathbf{H}^{-1})^T = [1 + D, D] \tag{4.33}$$

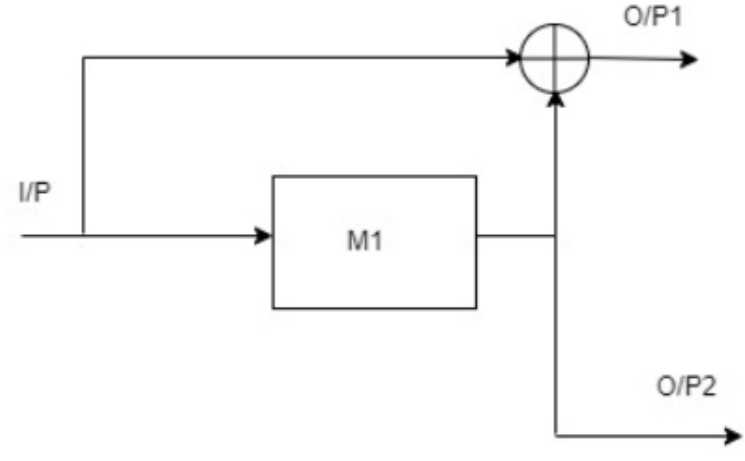

Figure 4.8: Inverse Parity Check Matrix for (19,29) Shaping Code

Bit error Probability for 16-state Trellis

Likewise, for the 16-state shaping code, the bit-error probabilities are calculated using the following parameters, rate=1/2, k=1, $B_{d_{free}}$ = 1, and d_{free}= 3. The bit-error probability $Pb_{s,f}$ for 16-state trellis are given as:

$$Pb_{s,f} \approx \frac{1}{2}(e^{\frac{S}{N}})^3 \tag{4.34}$$

4.4 Results and Discussion

Herein, we provided the simulation results to validate the effectiveness of our proposed technique. The simulation have been carried out in Matlab R2015a. For simulation results, we a consider a down-link PD NOMA-OFDM systems with a central base station feeding two users. Moreover, 16-QAM constellation with Gray Mapping, with $N = 128$ sub-carriers. Trellis shaping with (5, 7) 4-state shaping code is used for PAPR reduction in PD NOMA-OFDM system. The simulation counter is set to 1000.

For PD NOMA-OFDM down-link scenario, we consider two different scenarios to apply the TS, i.e.,

1. TS prior to the super position coding, i.e., doing trellis shaping on the individual users before the superposition coding.

2. TS after the SPC, i.e, applying TS shaping on one users data. For this scenario, TS is applied to one user whereas the data of the other user is provided and superposed and input to the TS for calculation of the path metric in the trellis of a shaping code.

4.4.1 First approach: TS prior to the SPC

A block diagram of TS prior to the superposition coding is as shown in Fig. 4.9. As shown in the figure, user $U1$ and user $U2$ data is passed through the trellis shaping block, individually. Superposition coding is applied after TS, i.e., over the shaped QAM symbols, to get a NOMA symbol. The NOMA symbols are then passed through a S/P converter followed by an IFFT modulator, which converts data into the time domain.

Figure 4.10 shows simulation results of the proposed scenario for PD NOMA-OFDM with 128 sub-carrier. It is obvious from the figure that a gain of 3.2 dB at 10^{-3} can be obtained with the proposed TS approach. However, the proposed gain is obtained at the expense of computational complexity as well as capacity loss. Subsequently, we propose our second

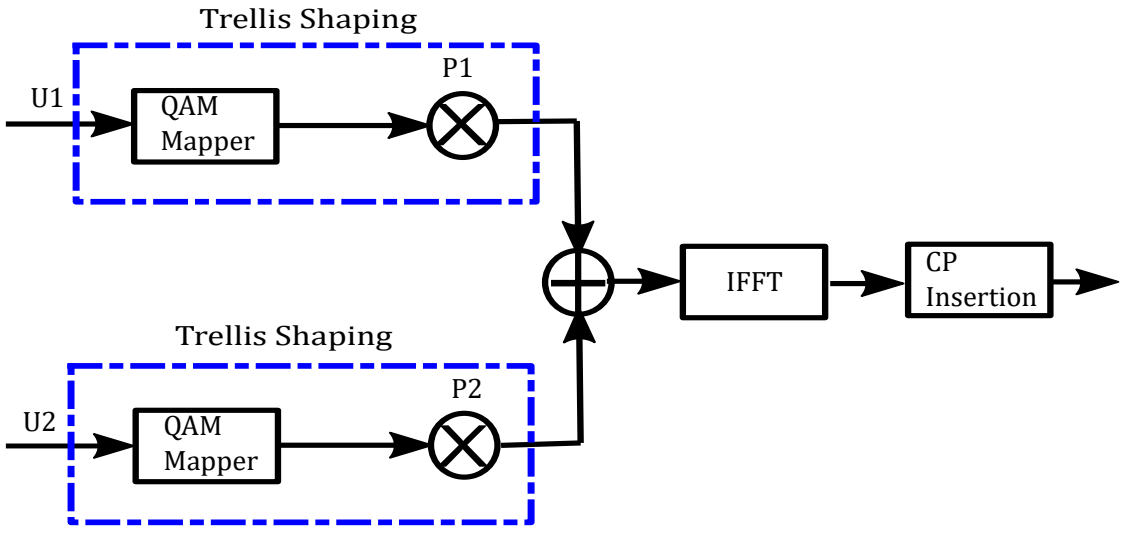

Figure 4.9: Block diagram of TS on both users

approach which has half the capacity loss as well as the computational as compared to the first approach.

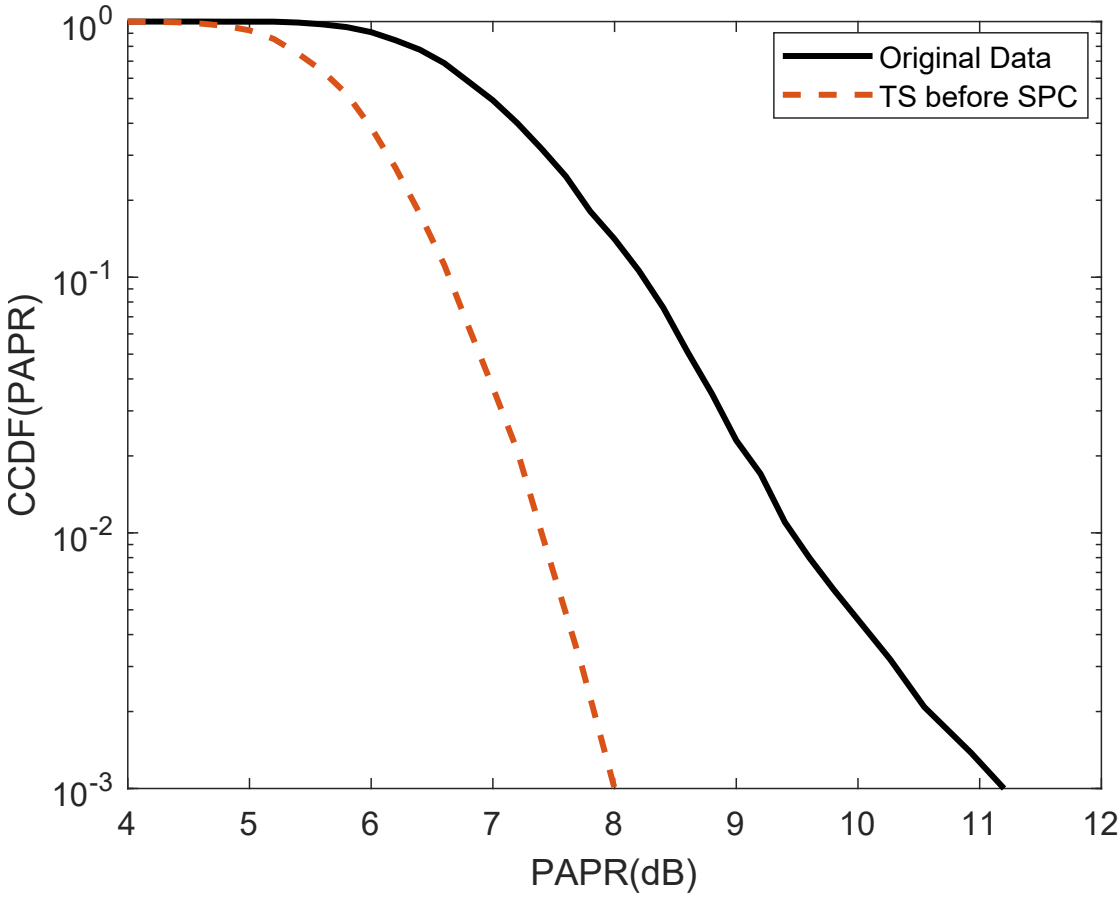

Figure 4.10: CCDF(PAPR) using TS prior to SPC

4.4.2 Second approach: TS on one user

TS can be applied on individual user in NOMA-OFDM, however, there are different parameters which needs to be considered. First, applying TS on individual user would mean addition of two redundant bits per NOMA symbol, i.e., a capacity loss of 2 bits per NOMA symbol. Applying TS on individual users is, therefore, spectrally in-efficient. Moreover, the computational complexity using TS on individual user is high, as the TS algorithm needs to be performed twice, once over each user. Besides that, there is a high possibility of peak regrowth when the users data is superposed. Peaks of the two signal may add up constructively resulting in peak regrowth.

An alternative approach will be to apply the TS algorithm on one user, as shown in Fig. 4.11. In the figure, TS is performed on user $U2$, whereas, the data of user $U1$ is super posed on $U2$ and is feed in to the TS. Thus, the effect of $U1$ is taken into account in the branch metric calculation of the shaping code. This approach has two benefits, first, one redundant bit is required per NOMA symbol. Therefore, it is spectrally more efficient as compared to the earlier approach. Second, since TS is performed on a single user, thus, the computational complexity of this approach is also half. Moreover, the effect of $U1$ is considered in the branch metric calculation, thus, the chances of peak regrowth is very low.

Figure 4.12 shows simulation results of the proposed scenario for PD NOMA-OFDM with 128 sub-carrier. It is obvious from the figure that a substantial gain of 2.8 dB at 10^{-3} can be obtained with the proposed TS approach.

4.4.3 Comparison of the two approaches

Figure 4.13 provides the CCDF curves for the proposed schemes. It is obvious from the figure that the first proposed approach, i.e., TS before SPC gives better results than the second approach. The gain obtained using the first approach, in terms of PAPR reduction,

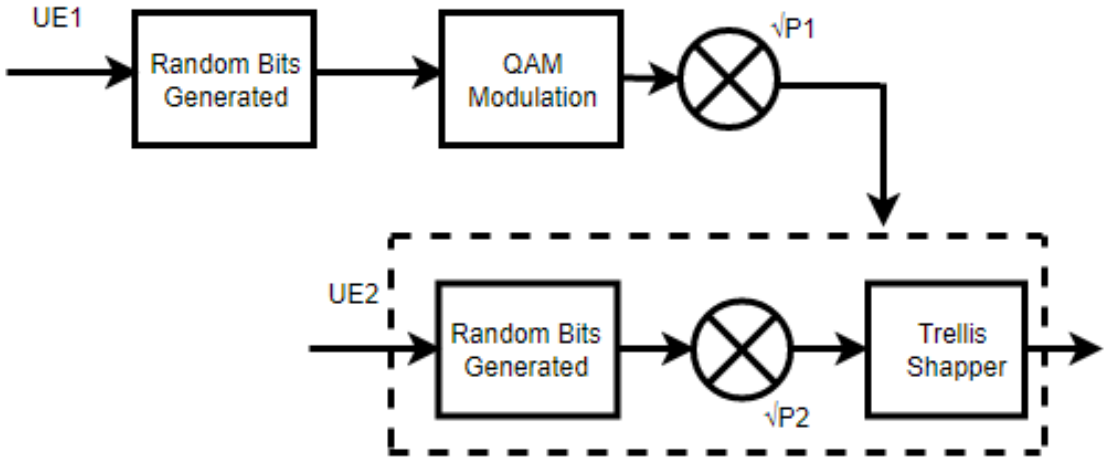

Figure 4.11: Block diagram of TS on one user

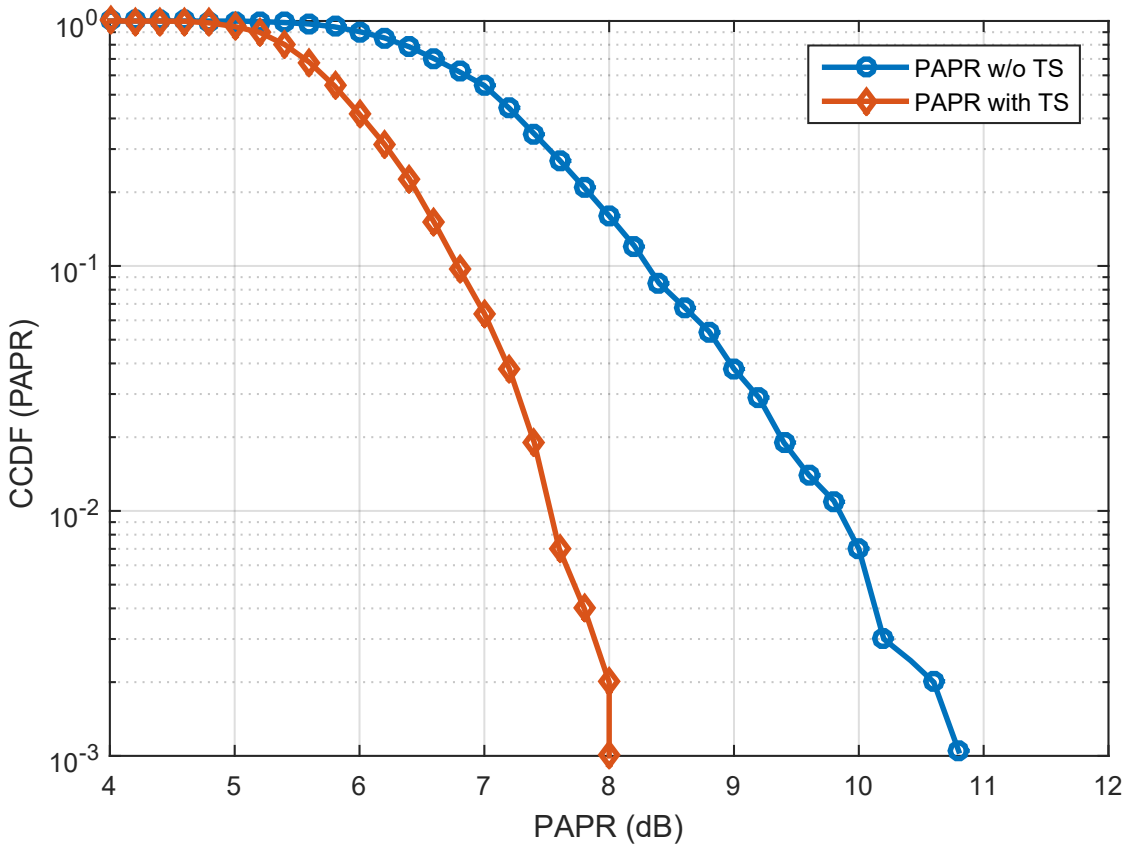

Figure 4.12: CCDF(PAPR) using TS after SPC

is 0.2 dB higher than the gain obtained with the second approach. However, the trade-offs for the superior performance of the first approach are; i) high computation complexity, as TS is performed on individual users and 2) Poor spectral efficiency, i.e., NOMA symbol has

two redundant bits, one bit per user which, thus, reduces it spectral efficiency. On the other hand, the second approach performs TS on one user, in this case on user $U2$. Therefore, the computational complexity is almost half as compared to the first approach. Moreover, in case of the second approach, only one redundant bit is added per NOMA symbol, thus, the capacity loss is also half as compared to the first approach.

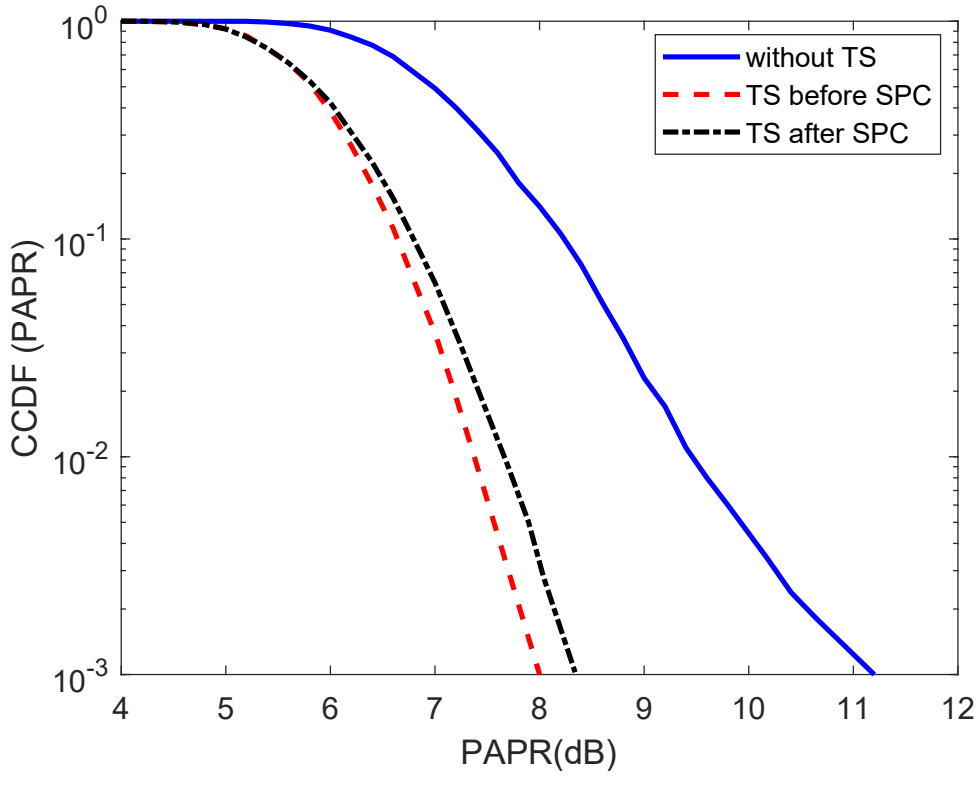

Figure 4.13: CCDF(PAPR) using TS of the proposed approaches

4.4.4 Trellis Shaping using higher states shaping codes

Forney demonstrated in his landmark paper [6], that the shaping gain can be increased by using shaping codes of higher constraint lengths, i.e, with higher number of states. However, it was mentioned in [6] that most of the gain can be achieved with a 4-state shaping code whereas the higher depths code can be used to improve the system performance. Herein, besides the 4-state shaping, we evaluate the performance of 8-states and 16-states shaping codes. Different parameters of the given codes is provided in given Table.

Shaping Codes	Number of States	Generator Matrix G	Inverse Syndrome Former H^{-T}	Syndrome Former H^{T}
(5,7)	4-State	$[1+D^2, 1+D+D^2]$	[D,1+D]	$[1+D+D^2, 1+D^2]$
(15,17)	8-State	$[1+D^2+D^3, 1+D+D^2+D^3]$	$[D+D^2, 1+D+D^2]$	$[1+D+D^2+D^3, 1+D^2+D^3]$
(19,29)	16-state	$[1+D^2+D^4, 1+D^2+D^3+D^4]$	[1+D,D]	$[1+D^2+D^3+D^4, 1+D^2+D^4]$

Figure 4.14: Parameters of Different Shaping Codes

Figure 4.15 shows the CCDF curves for TS using different shaping codes for PD NOMA-OFDM, with a window size $\Delta = 128$. It is clear from the figure that a gain of 2.8 dB can be obtained using a 4-state shaping code, whereas, the gain obtained using an 8-state shaping code is 3 dB. The system performance can further be enhanced using a 16-state shaping code with a gain of 3.2 dB. A 16-state shaping code outperforms the 4-state shaping code by 0.4 dB, however, this gain is obtained at the expense of additional computational complexity. The computational complexity of TS using a 16-states shaping code is almost 4 time that of the 4-state shaping code. Thus, the trade-off for the additional gain obtained is the computational complexity.

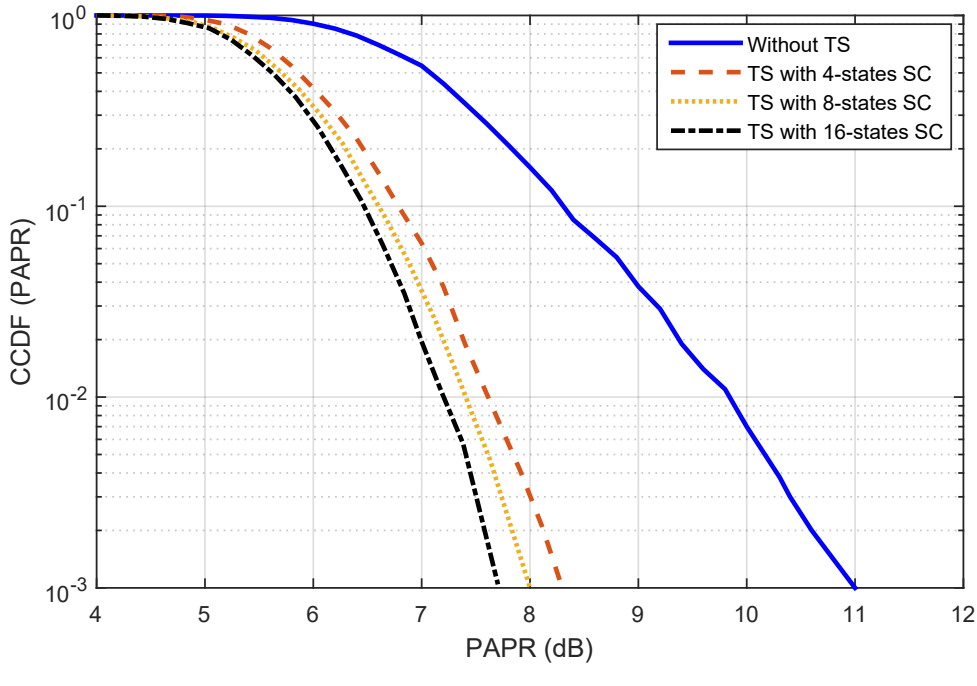

Figure 4.15: CCDF(PAPR) of different shaping codes, with the same window size, i.e., $\Delta = 128$

Chapter 5

Trellis Shaping Based Active Constellation Extension For PAPR Reduction in OFDM-Based NOMA

https://www.overleaf.com/project/630df45c89faf025db867424 AS discussed in the previous chapter, Trellis shaping has the capability for PAPR reduction in PD NOMA-OFDM systems without any increase in the mean power of the transmit signal. To further enhance the system performance, herein, we propose Active Constellation Extension (ACE) based Trellis shaping for PAPR reduction in NOMA-OFDM systems. Moreover, it has been found in the literature that shaping gain increases with the Trellis depth of the shaping code, therefore, to further improve the system effectiveness, shaping codes of different depths are suggested.

5.1 Active Constellation Extension

Another well known technique for PAPR reduction is Active Constellation Extension. IN ACE, the outer active constellation points are extend to lower PAPR. As shown in Fig. 5.1, The outer constellation points are extended in the outward direction using QPSK. The Euclidean distance between the constellation points grows as the constellation point are moved away from the origin. As BER is a function of Euclidean distance, besides the PAPR reduction, BER therefore, improves as well. It can be seen in the figure that as we extend any of the constellation points, the amplitude and phase change. In 16-QAM, the corner or outer constellation points have the option of reducing the PAPR. The feasible region is the comparable region fohttps://www.overleaf.com/project/62eb814c6ec6b9fed18d91aer the outer points. The constellation points near the centre of the constellation do not have the freedom to reduce the PAPR because extending them reduces the Euclidean distance between them, affecting BER.

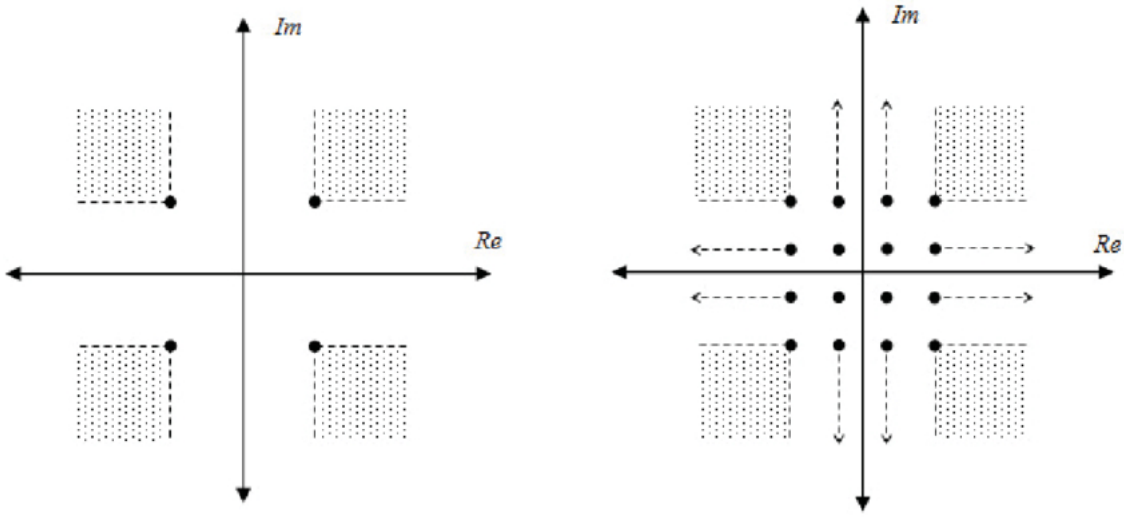

Figure 5.1: Active Constellation Extension

The disadvantage of this strategy is that, when expanding the points outwards the average power increases. Another drawback is that, as the constellation size grows larger, such as 64-QAM for higher order constellations, the inner points of the constellation lose their ability to lower the PAPR. However, there is a benefit in that no side information is necessary, resulting in no data rate loss. For modulations with a large constellation size, the average transmitted signal power has limited application in NOMA, therefore, ACE fits well for low data rates systems using 16-QAM constellation.

5.1.1 Metric Design for ACE for OFDM Signal

Discrete baseband form for OFDM in time-domain can be expressed as:

$$x_n = \frac{1}{\sqrt{N}} \sum_{k=0}^{N-1} X_k e^{j2\pi \frac{kn}{JN}} \qquad n = 0, \cdots, JN-1 \tag{5.1}$$

In order to reduce peak power of an OFDM symbol, ACE scheme adds distortion to the already modulated subcarriers. The distortion signal will be represented as:

$$\hat{x_n} = x_n + d_n = \frac{1}{\sqrt{N}} \sum_{k=0}^{N-1} (X_k + D_k) e^{j2\pi \frac{kn}{N}} \tag{5.2}$$

Where d_n and D_k represent the nth sample distortion and the kth subcarrier distortion, respectively. The PAPR is given to measure the degree of power variation as follows:

$$\varepsilon = \frac{max_{[n\in 0,JN-1]}\left|\hat{x_n}\right|^2}{E|x_k|^2} \tag{5.3}$$

The denominator in the preceding equation is the primitive that eludes variations in quantity of reference. This is triggered by the increase in signal power following the ACE. Because the average power in OFDM remains constant throughout the iteration, minimizing signal peaks can be simplified as a reduction in maximum power. The peak reduction is written as follows:

$$maximize_D||x + \mathcal{F}[D]||_\infty^2 \ , \tag{5.4}$$

where $x = [x_0, \cdots, x_{JN-1}]^T$, $D = [D_0, \cdots, D_{N-1}]^T$ and $\mathcal{F}$ denotes the IFFT operator.

5.2 Active Constellation Extension based Trellis Shaping:

As previously stated, one of the key disadvantage of an OFDM system is it's high PAPR, which limits its implementation in many wireless communication technologies. To overcome this problem multiple methods have been proposed by different authors in the literature with their pros and cons. Some of them have computational complexity such as SLM, PTS and some of them employing convex minimization, some of them cause disruption in the transmitted data such as clipping and filtering, some of them required reserved capacity such as tone reservation. ACE is one of the greatest strategies for ensuring that data is not disrupted during transmission.Extra information bits are not required for ACE or Trellis Shaping to be delivered with the sent data.. As we have already discussed that TS has low computational cost and it will not degrade the system's performance. Here we have proposed hybrid combination algorithm to reduce PAPR: TS based ACE. We have performed trellis shaping to reduce PAPR through minimization of auto-correlation of side-lobes and

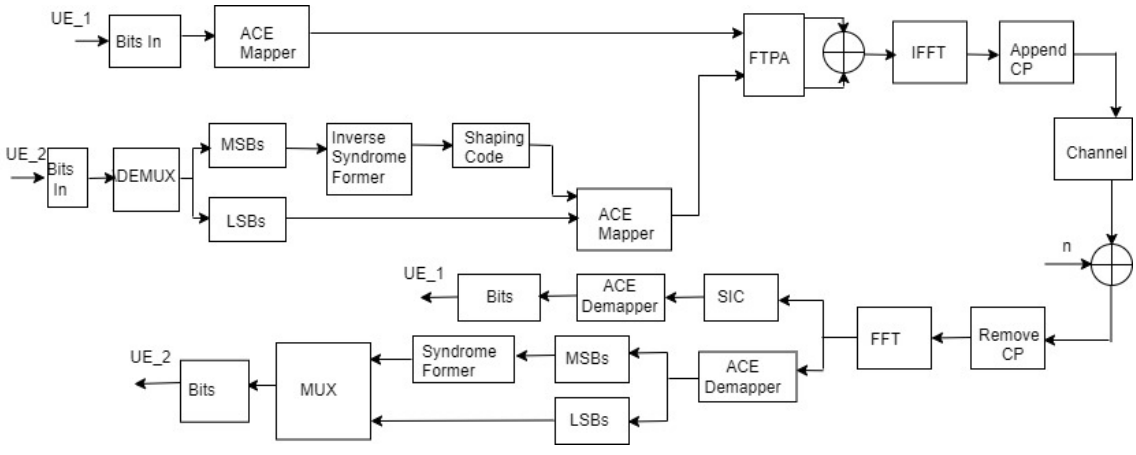

Figure 5.2: NOMA-OFDM Using ACE based TS

we have performed ACE to reduce PAPR by enlarging the outermost constellation points and convex minimization techniques are used to find an optimum solution. We have improved the system performance by using idea of constellation extension and using TS to minimize the autocorrelation of the side-lobes of the extended points with slight growth in complexity. ACE will degrade the performance by cancelling the peaks of the transmitted signal in time-domain.

5.3 Simulation Results

5.3.1 PAPR Reduction of Different Trellis Depths

In this section we have shown simulation results for PAPR of different trellis depths using ACE and TS based ACE for the proposed system. Here we have performed simulation for 16-QAM using 128 sub-carriers and using 1000 as a simulation counter.We have performed simulations using 4-state,8-state and 16-state trellis for the proposed system using ACE and using TS based ACE. We have seen that the using TS based ACE PAPR is better than using ACE. PAPR for highest state (16-state) is better as compared to the other states (4-state and 8-state).

Figure 5.3 shows the CCDF curves for NOMA-OFDM system using TS based ACE and TS without ACE for scenario 2, i.e., TS after super position coding. It is clear from the

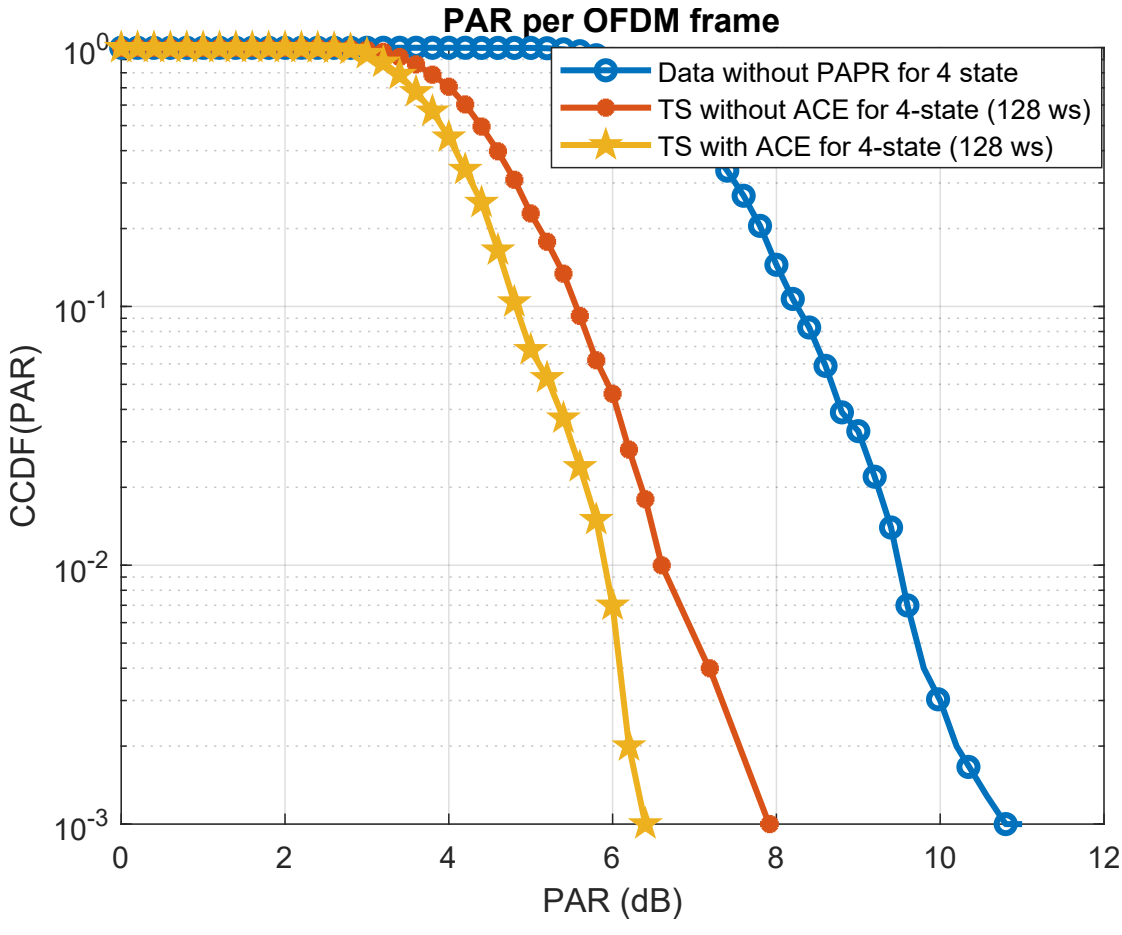

Figure 5.3: CCDF of PAPR for ACE based TS VS TS

picture that the PAPR of the NOMA-OFDM system can further be improved by approximately 1.6 dB using TS based ACE as compared to applying only TS. It is quite clear that using TS based ACE further improves the performance of NOMA-OFDM in terms of PAPR reduction.

5.3.2 Simulation Results for the Proposed Model using ACE with different shaping codes

Figure 5.4 shows the simulation results for ACE based TS with Δ=128 shaping codes of higher depths, i.e., with 8-state and 16-state shaping codes. The right most curve shows gain for 4-state trellis without PAPR Reduction. The Second curve form the right is for 4-state with TS only followed by 4-state ACE. It is obvious form the figure that the system performance can be improved using shaping codes of higher depths. A gain of 0.8 dB can be

achieved using a shaping code with 16-states as compared to using a 4-state shaping code. However, this gain is obtained at the expense of additional computational complexity.

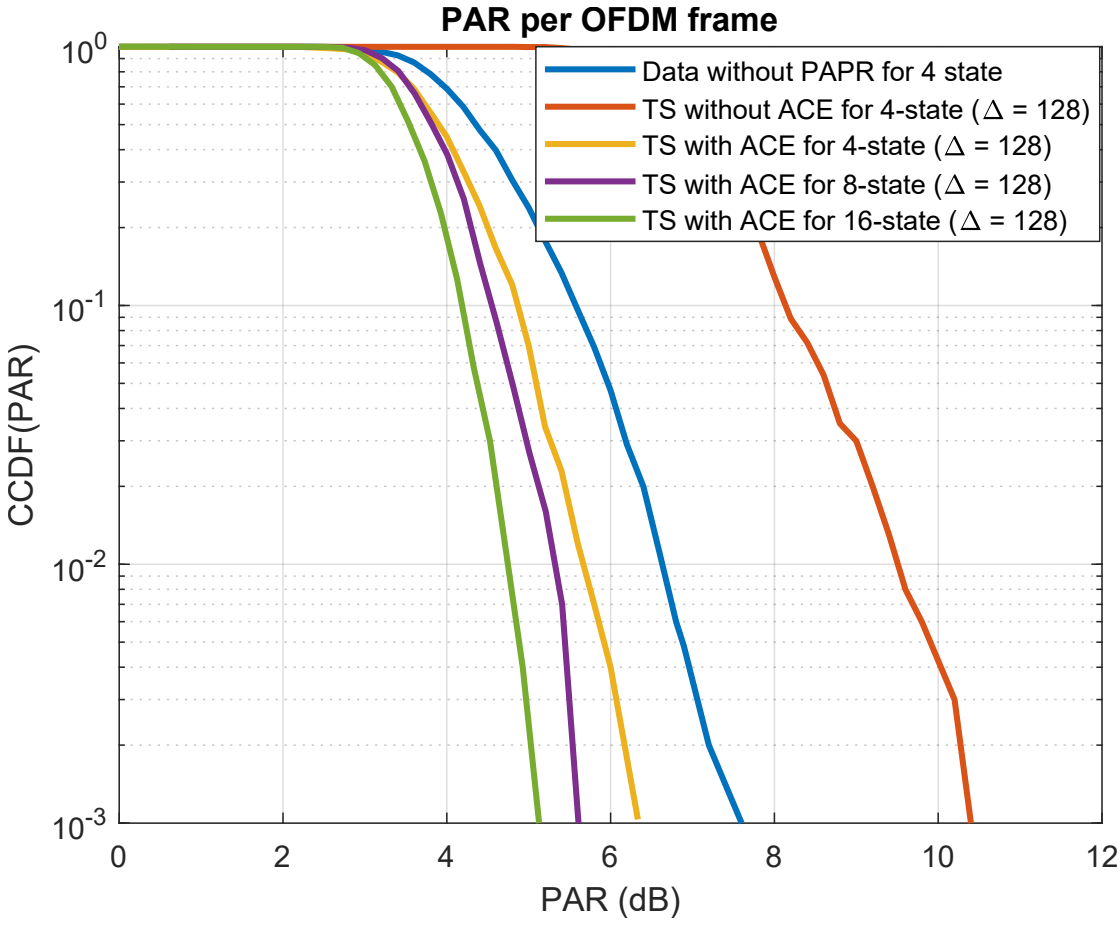

Figure 5.4: PAPR of ACE using same window size

Chapter 6

Conclusion and Future Work

6.1 Conclusion

Herein, Trellis Shaping is proposed to reduce PAPR in PD OFDM-NOMA systems. We have used shaping codes of various trellis depths. Using higher Trellis depths, system's performance is enhanced in terms of PAPR as shown in the simulation results. By using Trellis shaping we have a gain of almost 3dB. However, we get the gain at the cost of a slight increase in the system computational complexity. A hybrid algorithm based on Active constellation extension with trellis shaping is proposed for PAPR reduction in NOMA-OFDM systems. Using shaping codes for higher Trellis depths are analyzed using TS based ACE technique. Different Trellis depths with the same and different window size are analyzed. The simulation results show that using the proposed hybrid scheme will further enhance the effectiveness of TS for PAPR reduction in OFDM-NOMA systems.

6.2 Future Work

PAPR reduction using Trellis Shaping for higher constellation can be performed for the proposed model to improve system's performance in terms of PAPR. We have performed for 16-QAM in future we can use 64-QAM and 256-QAM. We can use higher trellis depths like 32-state Trellis to improve system's performance

Biblography

[1] K. Higuchi and A. Benjebbour, “Non-orthogonal multiple access (NOMA) with successive interference cancellation for future radio access,” IEICE Trans. Commun., vol. E98-B, no. 3, pp. 403–414, Mar. 2015.

[2] A. Benjebbour et al., “Concept and practical considerations of non-orthogonal multiple access (NOMA) for future radio access,” in Proc. IEEE Intell. Signal Process. Commun. Syst. (IEEE ISPACS), Naha, Japan, Nov. 2013, pp. 770–774

[3] Y. Du, B. Dong, Z. Chen, J. Fang, and X. Wang, “A fast convergence multiuser detection scheme for uplink SCMA systems,” IEEE Commun. Lett., vol. 5, no. 4, pp. 388–391, Aug. 2016.

[4] X. Li and L. J. Cimini Jr., ”Effects of clipping and filtering on the performance of OFDM”, Proc. IEEE Vehicular Technology Conf. (VTC’97), pp. 1634-1638, 1997-May.

[5] N. J. A. Sloane, “Tables of sphere packings and spherical codes,” IEEE Trans. Inform. Theory, vol. IT-27, pp. 327-338, 1981.

[6] G. D. Forney Jr., ”Trellis shaping”, IEEE Trans. Inform. Theory, vol. 38, pp. 281-300, Mar. 1992.

[7] W. Henkel and B. Wagner, ”Another application for trellis shaping: PAR reduction for DMT (OFDM)”, IEEE Trans. Commun., vol. 48, pp. 1471-1476, Sept. 2000.

[8] T. Peng and M. Ye, “PAPR mitigation in superposition coded modulated systems using selective mapping,” in International Conference on Computer and Communication Technologies, 2012, pp. 103–106

[9] L. Ping, J. Tong, J.X. Yuan and Q. Guo, “Superposition coded modulation and iterative linear MMSE detection,” IEEE Journal on Selected Areas in Communications, vol. 27, no. 6, pp. 995–1004, 2009.

[10] T. Jiang and Y. Wu, “An overview: peak-to-average power ratio reduction techniques for OFDM signals,” IEEE Transactions on Broadcasting, vol. 54, no. 2, pp. 257–268, 2008.

[11] I. Baig and V. Jeoti, “PAPR reduction in mobile WiMAX: A new ZCMT precoded random interleaved OFDMA system,” Journal of Central South University, vol. 19, no. 4, pp. 988–993, 2012.

[12] M. Park, H. Jun, J. Cho, N. Cho, D. Hong and C. Kang, “PAPR reduction in OFDM transmission using Hadamard transform,” in IEEE International Conference on Communications, 2000, pp. 430–433.

[13] I. Baig and V. Jeoti, “Zadoff–Chu matrix transform precoding-based orthogonal frequency division multiple access uplink systems: a peak-to-average power ratio performance,” Arabian Journal for Science and Engineering, vol. 38, no. 3, pp. 613–620, 2013.

[14] S.H. Muller and J.B. Huber, “OFDM with reduced peak-to-average power ratio by optimum combination of Partial Transmit Sequences,” Electronics Letters, vol. 33, No. 5, February 1997.

[15] J. Tellado and J.M. Cioffi, “Peak power reduction for multicarrier transmission,” Information Systems Laboratory, Stanford University.

[16] H. Ochiai, “A novel Trellis-Shaping design with both peak and average power reduction for OFDM systems,” IEEE Transactions on Communications, Vol. 52, No. 11 pp. 1916-1926, November 2004.

[17] Arsla Khan and Soo Young Shin (2017) Linear Precoding Techniques for OFDM-Based NOMA over Frequency-Selective Fading Channels, IETE Journal of Research, 63:4, 536-551, DOI: 10.1080/03772063.2017.1299045

[18] Tang, Tao, Yulong Mao, and Guangmin Hu. 2020. ”A Fair Power Allocation Approach to OFDM-Based NOMA with Consideration of Clipping” Electronics 9, no. 10: 1743. https://doi.org/10.3390/electronics9101743

[19] Reza Sayyari, Jafar Pourrostam, Hamed Ahmadi,”Efficient PAPR reduction scheme for OFDM-NOMA systems based on DSI and precoding methods”, Physical Communication,Volume 47, 2021,101372,ISSN 1874-4907, https://doi.org/10.1016/j.phycom.2021.101372.

[20] Vinay Kumar Trivedi, K. Ramadan, Preetam Kumar, Moawad Ibrahim Dessouky, Fathi E. Abd El-Samie,”Enhanced OFDM-NOMA for next generation wireless communication: A study of PAPR reduction and sensitivity to CFO and estimation errors”,AEU - International Journal of Electronics and Communications,Volume 102, 2019,Pages 9-24,ISSN 1434-8411,https://doi.org/10.1016/j.aeue.2019.01.009.

[21] Pandya S, Wakchaure MA, Shankar R, Annam JR. ”Analysis of NOMA-OFDM 5G wireless system using deep neural network”. The Journal of Defense Modeling and Simulation. March 2021. doi:10.1177/1548512921999108

[22] S. B. Weinstein, “The history of orthogonal frequency-division,” IEEE Communication Magazine, Vol. 47, pp. 26-35, November 2009.

[23] W. Y. Zou and Y. Wu, “COFDM- An overview,” IEEE Transactions on Broadcasting, Vol. 41, No. 1, pp. 1-8, March 1995

[24] L. Hanzo, M. M¨unster, B. J. Choi, and T. Keller, OFDM and MC-OFDMA for Broadband Multi-User Communicataions, WLANs and Broadcasting, John Wiley and sons Ltd., 2003.

[25] A. Goldsmith, Wireless Communications, Cambridge University Press, 2005.

[26] P. S. Chow, J. M. Cioffi, and J. A. C. Bingham “A practical discrete multitone transceiver loading algorithm for data transmission over spectrally shaped channels,” IEEE Transactions on Communications, Vol. 43, No. 2/3/4, pp. 773-775, April 1995.

[27] Tellado, Peak-to-average power reduction for multicarrier modulation, Ph.D. thesis, Stanford University, USA, September 1999.

[28] C. Siegel, Peak-to-average power reduction for multi-antenna OFDM via multiple signal representation, Ph.D. thesis, Friedrich Alexander Universit¨at Erlangen, N¨urnberg, Germany, 2010.

[29] K. S. Hassan, Unequal error protection adaptive modulation in multicarrier systems, Ph.D. thesis, Jacobs University Bremen, Germany, November 2011.

[30] A. D. S. Jayalath and C. Tellambura, "Reducing the out of band radiation of OFDM using an extended guard interval," IEEE Vehicular Technology Conference, New Jersy, USA, 2001.

[31] T. Lee and H. Ochiai, "Characterization of power spectral density for nonlinear amplified OFDM signals based on cross-correlation coffecient," EURASIP Journal of Wireless Communications and Networking, 2014.

[32] Tellado and J.M. Cioffi, "Peak power reduction for multicarrier transmission," Information Systems Laboratory, Stanford University.

[33] W. Henkel and V. Zrno, "PAR reduction revisited: an extension to Tellado's method," 6th International OFDM Workshop, Hamburg, Germany, September 2001.

[34] G. D. Forney, "Trellis Shaping," IEEE Transactoins on Information Theory, Vol. 38, pp. 281-300, March 1992.

[35] W. Henkel and B. Wagner, "Another application for Trellis Shaping: PAR reduction for DMT (OFDM)," IEEE Transactions on Communications, Vol. 48, No. 9, pp. 1471-1476, September 2000.

[36] T. T. Nguyen and L. Lampe, "On Trellis Shaping for PAR reduction in OFDM systems," IEEE Transactions on Communications, Vol. 55, No. 9, pp. 1678-1682, September 2007.

[37] S. Fei, Y. Yong, Z. Shijie, and S. Dechun, "A novel PAPR reduction with Trellis Shaping in NC-OFDM in cognitive radio," Journal of Electronics (China), Vol. 26, No. 3, pp. 296-302, May 2009.

[38] H. Ochiai, "A novel Trellis-Shaping design with both peak and average power reduction for OFDM systems," IEEE Transactions on Communications, Vol. 52, No. 11 pp. 1916-1926, November 2004.

[39] R. Yoshizawa and H. Ochiai, "A serial concatenation of coding and trellis shaping for OFDM systems with peak power reduction," IEEE International Symposium on Information Theory (ISIT), Cambridge, USA, July 2012.

[40] Y. Saito, A. Benjebbour, Y. Kishiyama, and T. Nakamura, "System level performance evaluation of downlink nonorthogonal multiple access (NOMA)," in Proc. IEEE Int. Symposium on Personal, Indoor and Mobile Radio Commun., London, UK, Sept. 2013.

[41]] Z. Ding, Z. Yang, P. Fan, and H. V. Poor, "On the performance of non-orthogonal multiple access in 5G systems with randomly deployed users," IEEE Signal Process. Lett., vol. 21, no. 12, pp. 1501–1505, Dec. 2014.

[42] J. Choi, "Power allocation for max-sum rate and max-min rate proportional fairness in NOMA," IEEE Commun. Lett., vol. 20, no. 10, pp. 2055–2058, Oct. 2016.

[43] S. Timotheou and I. Krikidis, "Fairness for non-orthogonal multiple access in 5G systems," IEEE Signal Process. Lett., vol. 22, no. 10, pp. 1647–1651, Oct. 2015.

[44] J. Choi, "Non-orthogonal multiple access in downlink coordinated two-point systems," IEEE Commun. Lett., vol. 18, no. 2, pp. 313–316, Feb. 2014.

[45] P. Pandey and R. Tripathi, "Performance Analysis of Peak-to-Average Power Ratio (PAPR) Reduction Techniques in an OFDM System," 2012 Third International Conference on Computer and Communication Technology, 2012, pp. 245-249, doi: 10.1109/ICCCT.2012.57.

[46] R. J. Baxley and G. T. Zhou, "Comparing selected mapping and partial transmit sequence for PAR reduction," IEEE Trans. Broadcasting, vol. 53, no. 4, pp. 797–803, Dec. 2007.

[47] G. D. Forney Jr., "Trellis shaping", IEEE Trans. Inform. Theory, vol. 38, pp. 281-300, Mar. 1992.

[48] D. Jones, "Peak power reduction in ofdm and dmt via active channel modification," in Conference Record of the Thirty-Third Asilomar Conference on Signals, Systems, and Computers (Cat. No.CH37020), vol. 2, 1999, pp. 1076–1079 vol.2.

[49] B. Krongold and D. Jones, "Par reduction in ofdm via active constellation extension," IEEE Transactions on Broadcasting, vol. 49, no. 3, pp. 258–268, 2003.

[50] G. Woo and D. Jones, "Peak power reduction in mimo ofdm via active channel extension," in IEEE International Conference on Communications, 2005. ICC 2005. 2005, vol. 4, 2005, pp. 2636–2639 Vol. 4

[51] C. Campopiano and B. Glazer, "A coherent digital amplitude and phase modulation scheme," IRE Trans. Commun., vol. 10, pp. 90–95, Dec. 1962.

[52] S-J Park, Triangular quadrature amplitude modulation. IEEE Commun. Lett. 11(4), 292–294 (2007)

[53] S-J Park, Performance analysis of triangular quadrature amplitude modulation in AWGN channel. IEEE Commun. Lett. 16(6), 765–768 (2012)

[54] K Cho, J Lee, D Yoon, Performance analysis of generalized triangular QAM. J. Korea Inf. Commun. Soc. (in Korean) 35(11), 885–888 (2010)

[55] TT DUY, HY KONG, A simple approximation for the symbol error rate of triangular quadrature amplitude modulation. IEICE Trans. Commun. 93-B(3), 753–756 (2010)

[56] KN Pappi, AS Lioumpas, KK George, -QAM: a parametric quadrature amplitude modulation family and its performance in AWGN and fading channels. IEEE Trans. Commun. 58(4), 1014–1019 (2010)

[57] L Jaeyoon, Y Dongweon, C Kyongkuk, Error performance analysis of M-ary -QAM. IEEE Trans. Veh. Technol. 61(3), 1423–1427 (2012)

[58] L. Hanzo, W. Webb, and T. Keller, Single- and Multi-Carrier Quadrature Amplitude Modulation. John Wiley and Sons, Ltd., 2000

[59] B.Ling, C.Dong, J.Dai, J.Lin. (2017). Multiple decision aided successive interference cancellation receiver for NOMA systems. IEEE Wireless Communications Letters, 6(4), 498-501.

[60] Yang, L., Liu, Y., Siu, Y. (2016). Low complexity message passing algorithm for SCMA system. IEEE Communications Letters, 20(12), 2466-2469.

[61] R. Sayyari, J. Pourrostam and H. Ahmadi, "A Low Complexity PTS-Based PAPR Reduction Method for the Downlink of OFDM-NOMA Systems," 2022 IEEE Wireless Communications and Networking Conference (WCNC), 2022, pp. 1719-1724, doi: 10.1109/WCNC51071.2022.9771812.

[62] Reza Sayyari;Jafar Pourrostam;Hamed Ahmadi; (2021). Efficient PAPR reduction scheme for OFDM-NOMA systems based on DSI amp; precoding methods . Physical Communication, (), –. doi:10.1016/j.phycom.2021.10137

[63] Khan, Arsla; Shin, Soo Young (2017). Linear Precoding Techniques for OFDM-Based NOMA over Frequency-Selective Fading Channels. IETE Journal of Research, (), 1–16. doi:10.1080/03772063.2017.1299045

[64] Jiang, T.; Wu, Y. An Overview: Peak-to-Average Power Ratio Reduction Techniques for OFDM Signals. IEEE Trans. Broadcast. 2008, 54, 257–268.

[65] R. Sayyari, J. Pourrostam and H. Ahmadi, "A Low Complexity PTS-Based PAPR Reduction Method for the Downlink of OFDM-NOMA Systems," 2022 IEEE Wireless Communications and Networking Conference (WCNC), 2022, pp. 1719-1724, doi: 10.1109/WCNC51071.2022.9771812.